



**UiT** The Arctic University of Norway

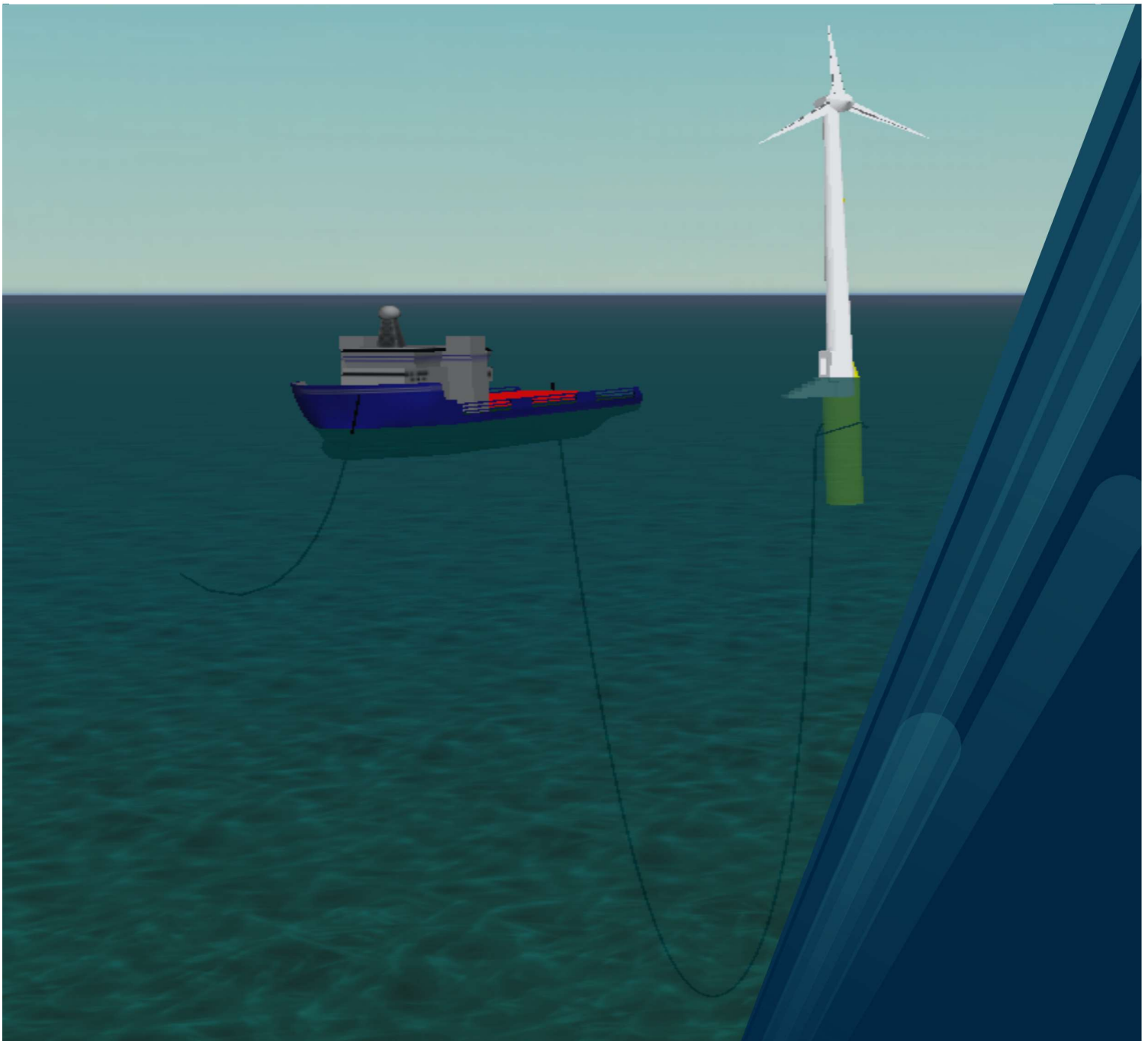
Faculty of Science and Technology

# **Towing of Floating Wind Turbine Systems**

**Rohith Jayachandran Nair**

TEK-3901 Master's Thesis in Technology and Safety

**Supervisor: Professor Egil Pedersen**



## **Acknowledgement**

I would like to thank Professor Egil Pedersen for being my supervisor and guiding me throughout the course of this thesis work. I thank Professor Javad Barabady with facilitating the lab access. Lastly, I am grateful to my wife Laura who amid this COVID 19 crisis supported me through my sudden unemployment and helped me to focus completely on my academics.

## **Abstract**

Towing is an important marine operation and floating wind turbines are the new way forward in our ever-expanding need for energy. In offshore floating wind turbine installation process, transport is an important phase. Presently, the turbines are assembled on shore and then towed to the installation spot one at a time. In this thesis, the theory behind the towing operation, modelling and simulation of various towing scenarios are carried out and the mathematical basis of the analysis is studied. It discusses previous research work that has been published in similar operations. The modeling and simulation has two different scenarios. In the first scenario is to find the optimum tow-point for the towing operation. It was found that it varies slightly with sea state but closer to center of buoyancy is optimal. In the second scenario, the simulation aims to find the scope of towing multiple turbines during a single tow-operation. In the process line tension was checked for a single turbine at different towing speeds. It was found that it is unfeasible to tow multiple turbines.

## Nomenclature

$D [m]$	:	<i>Cylinder outer diameter</i>
$P_{ex} [kN]$	:	<i>Total horizontal force</i>
$P_{ez} [kN]$	:	<i>Total vertical force</i>
$M_{0t} [kNm]$	:	<i>Overturning moment</i>
$C_h [-]$	:	<i>Horizontal Flow Coefficient</i>
$C_v [-]$	:	<i>Vertical flow Coefficient</i>
$F_{xk} [kN]$	:	<i>Froude-Krylov force horizontal</i>
$F_{zk} [kN]$	:	<i>Froude-Krylov force vertical</i>
$H [m]$	:	<i>Wave height</i>
$\gamma [-]$	:	<i>Dynamic Load factor</i>
$k [m^{-1}]$	:	<i>Wave number</i>
$C_m [-]$	:	<i>Inertia Coefficient</i>
$u [ms^{-1}]$	:	<i>water particle acceleration</i>
$F_a [kN]$	:	<i>Drag Force</i>
$U [ms^{-1}]$	:	<i>Instantaneous particle velocity</i>
$\rho [kgm^{-3}]$	:	<i>Density</i>
$v [ms^{-1}]$	:	<i>Cylinder velocity</i>
$V [ms^{-1}]$	:	<i>Fluid velocity vector</i>
$\Phi [m^2s^{-1}]$	:	<i>Velocity potential</i>
$i,j,k [-]$	:	<i>Unit Vectors in x, y and z directions</i>

$p [Nm^{-2}]$	:	<i>Pressure</i>
$z [m]$	:	<i>Depth</i>
$U_r [ms^{-1}]$	:	<i>Average wind velocity at reference height</i>
$A_p [m^2]$	:	<i>Horizontal projected area</i>
$\xi [ms^{-1}]$	:	<i>Vertical velocity of sea surface</i>
$\eta [ms^{-1}]$	:	<i>Vertical velocity of the structure</i>
$C_s [-]$	:	<i>Slamming coefficient</i>
$F_p [kN]$	:	<i>Propeller Thrust</i>
$u_o [ms^{-1}]$	:	<i>Flow velocity</i>
$D_p [m]$	:	<i>Propeller outer diameter</i>
$G_{xyz} [-]$	:	<i>Global coordinate system</i>
$B_{xyz} [-]$	:	<i>Buoy coordinate system</i>
$K_a [-]$	:	<i>Von-Karman's constant</i>
$z_0 [-]$	:	<i>Terrain roughness parameter</i>
$C_L [-]$	:	<i>Lift coefficient</i>
$F_t [N]$	:	<i>Fluid Force</i>
$\Delta [kg]$	:	<i>Fluid mass displacement</i>
$a_f [ms^{-2}]$	:	<i>Fluid acceleration relative to earth</i>
$C_a [-]$	:	<i>Added mass coefficient</i>
$a_r [ms^{-2}]$	:	<i>Fluid acceleration relative to body</i>
$v_r [ms^{-1}]$	:	<i>Fluid Velocity relative to body</i>

$d_{so} [m]$	:	<i>Spar outer diameter</i>
$d_{si} [m]$	:	<i>Spar inner diameter</i>
$t_s [m]$	:	<i>Wall thickness of spar</i>
$A_s [m^2]$	:	<i>Spar cross-sectional area</i>
$d_{t0} [m]$	:	<i>Tower outer diameter</i>
$d_{ti} [m]$	:	<i>Tower inner diameter</i>

# Table of Contents

Acknowledgement.....	2
Abstract .....	3
Nomenclature .....	1
1 Introduction .....	8
1.1 Objectives .....	10
1.2 Motivation .....	10
1.3 Literature Survey .....	11
1.3.1 Numerical investigation on nonlinear dynamics of a towed vessel in calm water 11	
1.3.2 Turning ability of ship towing system.....	12
1.3.3 Course Stability of a Ship Towing System .....	13
1.3.4 Modelling the Towline .....	13
1.4 Ongoing projects in floating wind turbine technology.....	14
1.4.1 Hitachi HTW 2.0 .....	14
1.4.2 Deepwind .....	14
1.4.3 EOLINK.....	15
1.4.4 PivotBuoy.....	15
1.5 Structure of the thesis .....	16
2 Theory .....	17
2.1 Wave loads on thin long floating cylinder.....	17
2.1.1 Froude-Krylov forces .....	17
Froude-Krylov Forces .....	17
2.1.2 Morison equation.....	19
2.2 Sea environment .....	22
2.2.1 Waves: Linear wave potential theory.....	22

2.2.2	Wind effects .....	26
2.2.3	Current effects .....	27
2.2.4	Slamming force .....	27
2.3	Floating wind turbines .....	28
2.3.1	Spar buoy type wind turbine .....	28
2.3.2	Tension leg platform type .....	29
2.3.3	Pontoon type.....	30
2.3.4	Semi-submersible type wind turbine.....	31
2.4	Hywind Scotland wind turbines .....	31
2.5	Marine towing operations.....	34
2.5.1	Towline.....	35
2.5.2	Towing gear.....	37
2.5.3	Propeller wash effect.....	39
3	Modelling theory .....	41
3.1	Orcaflex theory and modeling .....	41
3.1.1	Coordinate system and object connections .....	41
3.1.2	Environment.....	42
3.1.3	6D buoy theory.....	43
3.1.4	Line theory .....	45
3.1.5	Dynamic analysis .....	46
	Frequency domain .....	46
	Time domain dynamic analysis.....	46
3.1.6	Object modelling.....	47
4	Modelling and simulation technique .....	51
4.1	Setup and assumptions.....	51
4.2	Environmental data.....	51
4.3	Spar buoy/ Floating wind turbine .....	52



4.3.1	Ballast mass and submerged area.....	53
4.4	Towline model.....	56
	Mass-Spring-Damper model of towline. ....	56
4.4.1	.....	56
4.5	Other objects.....	57
5	Simulation and results .....	58
5.1	Tow point vs pitch angle .....	58
5.2	Tow speed vs line tension.....	62
6	Concluding Remarks .....	64
	Works cited .....	65
	Appendix .....	67
1:	Turbine lean angles vs tow point at zero sea state .....	67
2:	Turbine lean angle vs Tow-point in sea-state 6 .....	69
3:	Wavelength for a given sea-state at a water depth ‘h’ .....	72

## List of Tables

Table 1:	Cost Distribution of a Wind Turbine. ....	11
Table 2	Hywind Demo and Scotland particulars (Equinor).....	34
Table 3:	Minimum Required Towline Breaking loads (RTBL).....	36
Table 4:	DNVGL-ST-N001 clauses.....	38
Table 5:	Environmental Parameters. ....	52
Table 6:	Wind turbine Characteristics.....	53
Table 7:	Towline parameters.....	56

## List of Figures

Figure 1	DeepWind floating wind turbine concept. (DeepWind).....	14
Figure 2	Eolink tubine concept. (Eolink).....	15
Figure 3:	PivotBouy Floating wind turbine concept (Xwind).....	16
Figure 4:	Diffraction Wave loading on submerged cylinder or box <sup>[5]</sup> .....	17

Figure 5: Fixed cylinder in Water .....	20
Figure 6 Spar bouy type Wind Turbine <sup>[9]</sup> .....	28
Figure 7 : Tension Leg Platform type Wind Turbine <sup>[11]</sup> .....	30
Figure 8: Pontoon Type wind turbines .....	30
Figure 9: Semi-Submersible type Wind Turbine (Li Liang et al) .....	31
Figure 10 Hywind Turbine.....	32
Figure 11: Supply vessel Power vs BP (Nielsel 2007).....	37
Figure 12: Tug arrangements (Navalarch.com) .....	37
Figure 13: Propeller wash deflection (Nielsen, 2007).....	40
Figure 14: Coordinate system used in orcaflex .....	42
Figure 15 Lumped buoy .....	44
Figure 16 Spar buoy .....	45
Figure 17: Vessel Data Form (OrcaFlex).....	47
Figure 18: Roughness parameters <sup>[7]</sup> .....	48
Figure 19: Deflector .....	49
Figure 20: System model.....	51
Figure 21: Permanent ballasting arrangement (LKAB minerals) .....	55
Figure 22:Turbine Spar data form.....	55
Figure 23: Mass-Spring-Damper model of a towline.....	56
Figure 24: Ramping function (Orcina).....	59
Figure 25: Turbine rotaion output at z=0 .....	59
Figure 26: Comparision of Tow point vs Pitch angle at sea-state = 0.....	60
Figure 27: Comparison of Tow point Vs Pitch angle at sea state = 6 .....	60
Figure 28:Sea state 0 vs Sea State 6 .....	61
Figure 29: Comparison of mass forces, viscous drag and diffraction forces on marine structures. (Faltinsen,1990).....	61
Figure 30: Tow speed Vs Force on the Towline. ....	62
Figure 31: Tow line tension at 1 m/s speed.....	63

# 1 Introduction

Humanity is realizing the fact that decades of industrial activity with fossil fuel as its backbone has run its course and needs a change. Conventional, non-renewable source of energy has always been a source of concern for humans. They are energy dense and applications are manifold. In an average household, numerous items from toothbrush to the heating iron to the fuel in the car as its origins in petroleum. In recent decades it's a well-known fact that our planet is warming up and the acidity of ocean has been on the rise. This has to do mainly with emissions which are a byproduct of using petroleum-based fuels. According to United nation's Inter governmental panel of climate change, unless fossil fuels are phased out, which includes petroleum, there will be "severe, pervasive, and irreversible impacts for people and ecosystems" [1]

Climate change is brought about a new thought process wherein the renewable energy takes precedence over conventional fuels. World is adapting to this change at a rapid pace and expected to adopt renewable energy at a faster rate in coming years. The renewables capacity is set to expand by 50% between 2016-2026. Out of which 60 % will be from solar power. Offshore wind will take up about 4% of the overall capacity but tripling in size by 2024.

Onshore wind turbines are generally unpopular thanks to their imposing size and noise generated. One of the positive factors for offshore system is the presence of strong wind which could be lacking sometimes for the onshore counterparts. So far, the main limiting factor for the offshore systems was the installation cost and depth limits. Installation costs, like any new technology will come down with time and with scale of production. Meanwhile, depth restrictions are always a problem for the conventional offshore wind turbines. The turbines are supported by structures that are anchored to the seabed. For the supported turbines, the depth of up to 45 meters has been tested and found working. This problem is what offshore floating turbines are trying to overcome. They are held up or supported by buoyancy of the subsea part they have. And hence, theoretically depth should not be a limiting factor for such turbines. This will also mean that they can be towed to a location beyond horizon and away from the local populace.

World's first commercial floating wind farm was installed in Peterhead, Scotland in 2015 and commissioned in 2017. It was a venture co-owned by Equinor AS of Norway and Masdar of Abu Dhabi. The system is fully developed by Equinor. From 2009 to 2015 the system was

installed under test conditions at Karmøy, Norway. After six years, the project moved on to second phase and was installed 29 km off the coast of Scotland. The turbines were assembled on shore and towed to the installation point vertically by ballasting the vertical substructure. In 2017 the 5 turbines were commissioned and has been operational. There are 5 turbines in the network each producing 6 MW each, total 30 MW nameplate capacity theoretically for the system.

During installation of such a system, towing or transporting the turbines is an important part of the whole enterprise. This project investigates the towing aspect of the system and tries to model the towing of multiple turbine at once, as opposed to one at a time system presently used.

Wind energy has its advantages and disadvantages. Biggest disadvantage faced by any wind power project, be it offshore or onshore system is the availability of reliable wind, along with the secondary hassle of noise pollution and aesthetic aspect of the structures. This is where offshore wind farms come into its element. They tend to be situated away from localities of inhabitation and to a certain extent away from sight. Denmark is the European leader in offshore wind farms. Wind Power contributed about 47 % of Denmark's total electricity consumption for the year of 2019 (*Reuters*) and plans have been adopted by the government to increase it to increase to 50% by 2020 and to 84% by 2035 (*The Guardian*) . One of the hurdles with offshore wind farms is the depth restrictions that they have. They are limited to 30 m of depth. Offshore floating wind farms on the other hand, theoretically, have no such restrictions (*Equinor*).

Offshore wind turbines are wind turbines that are floating at sea, anchored to a point. They can operate at very large depths and can be installed far away from the coastline. In 2009, Statoil of Norway installed a technology demonstrated in Karmøy, Norway. These had 2.3 MW capacity and blade diameter of 85 meters. The testing went on until 2015 without any incident. In 2015, Statoil got the permission to install the world's first commercial float wind farm off the coast of Petershead.

An important phase in installation of a floating wind turbine is the transportation phase. The towers are transported horizontally first. Once at assembly point, the spar structure is filled with sea water to weight them down and make the structure upright. Later, solid ballast

(concrete) is added while pumping out the sea water. Generator and wind rotor are mounted on the tower at the shore and then towed out to the sea using a tow ship.

## **1.1 Objectives**

The aim of this thesis is studying the behavior of towing operation of floating wind turbines by modelling and simulation utilizing the Orcaflex software. Specifically, with regards to a turbine model which is similar to Hywind Scotland Floating Wind turbines. The objectives are.

- 1. Study the lean angle variations with regards to varying tow-points on single wind turbine towing operation.**
- 2. Study the tow-speed versus towline tension.**
- 3. Study the feasibility of towing multiple wind turbines due to loads experienced by the tow vessel and the line.**

## **1.2 Motivation**

An offshore windfarm is an expensive proposition with multiple risk factors. One of them is the economic risk faced by the companies in-charge of installation operation of the wind turbines. The only operational floating wind farm, Hywind Scotland, has been supported by the UK Renewable Obligation Center subsidy scheme. As per this scheme the project by Statoil received £140/MWh to help recover the cost. UK government has since then shut down the subsidy scheme, thereby making it harder for future pilot project to take off. At present only France, Japan, Portugal, United States and Norway has promised support or planning support for the floating windfarms. With the prices of bottom fixed offshore wind slowly coming off the subsidies, the floating wind industry is fighting an uphill battle.

This thesis could help in minimizing the mechanical damage risk involved to generator by identifying the optimum conditions for the towing operation. For a Repower MM92 turbine with 45.3 m blade length and a 100 meter tower, following is the cost breakdown (EWEA 2007).

<b>Component</b>	<b>Percentage cost</b>
Tower	26.3%
Rotor Blades	22.2%
Rotor hub	1.4%
Rotor Bearings	1.2%
Main Shaft	1.9%
Main Frame	2.8%
Gearbox	12.9%
Generator	2.4%
Yaw System	1.3%
Pitch System	2.6%
Power Converter	5.0%
Transformer	2.6%
Brake System	1.3%
Nacelle housing	1.3%

*Table 1: Cost Distribution of a Wind Turbine.*

As seen from Table 1, more than half of the turbine cost is taken up by the nacelle assembly which includes components like gearbox, generation, bearing, main shaft etc. Minimizing undesirable loading while transport will enable designers to reduce the design load limits, thereby reducing the expenses.

## **1.3 Literature Survey**

### **1.3.1 Numerical investigation on nonlinear dynamics of a towed vessel in calm water**

Bo Woo H (2020), investigated the nonlinear dynamic response of a towed vessel in calm water. In this study the vessel was passively towed by a tug or a towline. A 3DOF mathematical model was used to derive the nonlinear dynamics of the towed vessel. The model was after a modular type hull force model which included 3<sup>rd</sup> order linear and non-linear damping forces in sway and yaw directions. In this study the tow line was modelled as

a linear spring. Sway and yaw coupled motions of the tow system caused by unstable towing characteristics was studied using phase plane analysis. The simulation results were directly compared to the model test data. Later the limit cycles were investigated by changing the parameters like tow speed, hull force coefficient and initial positions.

In this study it was found that the dynamic characteristics of the towed vessel come close to being chaotic due to nonlinear stiffness of the towline and motion of tug. The towing stability conditions are affected by the hull geometry, towline and tug systems and towing conditions. Research was based on the characteristic equations derived by Strandhagen et al (1950), Abkowitz (1964) and Bernitas (1985). They explained there are two conditions for stability,

1. Restoring moment conditions

The towed structure is hydrodynamical stable if restoring force due to lateral hydrodynamic moment is greater than yawing moment.

2. Minimum resistance condition

The towline tension corresponding to ship resistance should be larger than a critical value

The phase plane analysis demonstrated that the dynamic system of towed vessel has a stable limit cycle. The limit cycle showed that the lateral velocity and yaw rate had almost twice the oscillation period of surge velocity. High tension peaks occurred on the towline, whenever the vessel changed its heading. Second observation was that the towing phase trajectories were significantly affected by hull hydrodynamic force coefficients. And thirdly, it was found that nonlinear stiffness of the towline and the motion of the tug cause dynamic characteristics of the towed vessel come close to being chaotic.

### **1.3.2 Turning ability of ship towing system**

Fitriadhy and Yasukawa (2016) did the linear and nonlinear analysis for the turning ability with tug and a barge <sup>[3]</sup>. The effect of various parameters like the towline length, tug size, distance of town point from the center of gravity etc. were investigated. It was found that longer towline, larger tug and tow point away from center of gravity towards the bow increased the turning diameter. Whereas the tow points closer to the center of gravity decreased the turning diameter significantly.

This paper considered the coupled maneuvering motion equations of tug and towed barge in surge, sway and yaw. A 2D lumped mass method was applied to model the towline motion. This method allowed detecting horizontal deflections on any section of the towline segment and capturing any slack in the towline.

### **1.3.3 Course Stability of a Ship Towing System**

Along with their study mentioned in 2.2, A. Fitriadhy and H. Yasukawa also proposed a numerical model on course stability of towed ship-tow ship-towline system using linear and nonlinear approach.<sup>[4]</sup> The effects of towed ship, both stable and unstable, towline, the tow points, dimensions of the tow ship and autopilot rudder were considered in the analysis.

Their result showed longer towline, moving tow point closer to the bow made both stable and unstable ship more a more stable towing system. Lateral motion of the tow ship increased gradually due to the shifting of tow point towards the forward of the ship's center of gravity. This impacted the course stability of the system. It tended more and more towards being unstable. The motions were corrected by the inputs from the autopilot rudder. It was found that increasing the tow ship's dimensions were not enough to improve the course stability of the system.

### **1.3.4 Modelling the Towline**

Various models and assumptions have been made throughout regarding the towline used in the studies. In all these studies the towed ship and tow ship were considered decoupled. Yaskawas et al (2006) used 2D lumped mass method where the towline was divided into number of nodes and each node had its own equations of motion, while Bernitsas (1985,1986) and Lee (1989) used single elastic tow rope model. Kijima & Varyani (1985) used an approximate formula estimate towline system and assumed it to be straight and rigid, and Standhagen et al (1950) assumed a constant towline tension in analyzing course stability of the towed vessel, Nonaka (1990) and Yukaiva et al (2002) used single elastic tow rope model, and Bo Woo Ham (2020) used a linear spring model for the towline in his study.



## 1.4 Ongoing projects in floating wind turbine technology

### 1.4.1 Hitachi HTW 2.0

This is Japan's first floating offshore wind turbine. It was tested between 2010 and 2015 off the coast of Kabashima island. After the test period, the device was relocated to a position off the coast of Fukue island and has been named Sakiyama Floating 2MW wind turbine. The turbine is on a hybrid spar foundation which is moored using a 3-point catenary system. The whole structure is on 3 400 tonnes and of 172 meters in length.

### 1.4.2 Deepwind

Deepwind is a European project launched in October 2010 with a consortium of 12 international members.

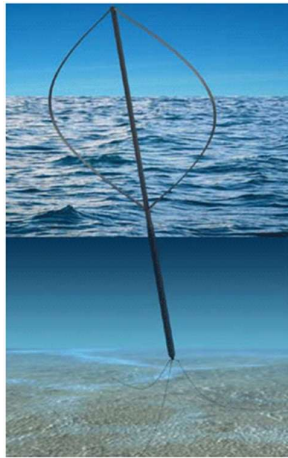


*Figure 1 DeepWind floating wind turbine concept. (DeepWind)*

Deepwind has a completely new offshore wind turbine concept. In this the turbine axis is vertical<sup>[15]</sup>. Numerous innovations are to be made to make this project a reality. These include,

1. New numerical tools for prediction of energy production, dynamics, loads and fatigue.
2. The innovative blade design will need research into production facilities and tooling.
3. Tools for design of generator and controls
4. Designing mooring and torque absorption system

### 1.4.3 EOLINK

Eolink is a prototype floating wind turbine installed at Finistere, France. The structure is 1/10 scale model of the intended design. The peculiarity of this design is that the conventional tower is replaced by four arms to reduce the mass and improve the structural resistance. This allows installation of large rotors despite the smaller supporting mass. The turbine is expected to produce 12 MW. The structure is installed on a semi-submersible steel/ concrete floater. The concept was developed at Plouza technopole (Finistere then tested at IFREMER, which partners the project. During the test, the model was subjected to many sea states, ranging from regular swell to focused waves and in presence of uniform or turbulent wind of up to 9 m/s.



*Figure 2 Eolink turbine concept. (Eolink)*

### 1.4.4 PivotBuoy

PivotBuoy is a system developed by the company 'X1 Wind'. It is a single point mooring system platform which in theory can reduce cost of floating offshore wind turbine systems. It is a consortium of 9 companies led by X1 Wind. They will be deploying a prototype at a test site in Canary Islands. The systems combine the concept of single point mooring system and tension leg platform system. The PivotBuoy concept is a downwind turbine and rotor configuration. This project uses a converted Vestas V27 225 KW upwind turbine used in a downwind configuration. The single point mooring system allows the floating platform to align itself to the wind, thereby eliminating the need for active ballast controllers.

The mooring system are electrical connections are pre- installed on site whereas the platform and turbine are fully assembled in port and towed to the location.



*Figure 3: PivotBouy Floating wind turbine concept (Xwind)*

## **1.5 Structure of the thesis**

Following is the structure of the thesis:

Chapter 1 introduces the background information that led up to the development of floating wind turbines, past studies in marine towing operations, enlists the objectives and mentions some of the future project in development.

Chapter 2 discusses the theory behind the effect of waves on a floating object. In this the Linear wave theory, Morison's equation and Froude-Krylov forces are explained. The environmental effects like waves, current and wind are discussed. The concept of floating wind turbine and marine towing operation is explained.

Chapter 3 discusses the OrcaFlex software and the background process that the software conducts to run the simulations. Different modelling objects in Orcaflex are looked into.

Chapter 4 explains the modelling scenarios used, assumptions and simplifications made. The modelling process in the software is mentioned.

Chapter 5 explains the simulation scenarios done and the result obtained. The results are discussed while conclusions and recommendation for further work are stated in Chapter 6.

## 2 Theory

### 2.1 Wave loads on thin long floating cylinder

#### 2.1.1 Froude-Krylov forces

In fluid dynamics, Froude-Krylov force is a hydrodynamic force caused by unsteady pressure field generated by undisturbed waves. This together with diffraction force make up the total non-viscous forces acting a floating body in a regular wave. Diffraction force is cause due to the floating body disturbing the waves

Diffraction force calculations are based on the Froude-Krylov pressure forces derived from the ideal, hydrodynamic flow and linear wave theory. These forces are modified experimental flow coefficients. The basic assumptions in the calculation of the Froude-Krylov forces is that the wave pressure field is completely undisturbed by the presence of the structure.

#### Froude-Krylov Forces

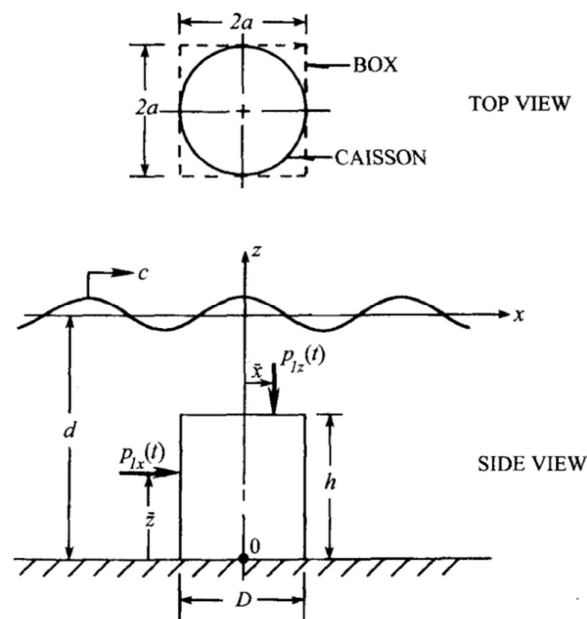


Figure 4: Diffraction wave loading on submerged cylinder or box <sup>[5]</sup>

Total horizontal force  $P_{1x}(t)$ , vertical force  $P_{1z}(t)$  and overturning moment  $M_0(t)$  of a single submerged column cylinder,

$$P_{1x}(t) = C_h F_{xk} \quad 1(a)$$

$$P_{1z}(t) = C_v F_{zk} \quad 1(b)$$

$$M_0(t) = C_0 (z F_{lk} + x F_{zk}) = C_0 M_k \quad 1(c)$$

$C_h$ ,  $C_v$  and  $C_0$  are respective flow coefficients.

$F_{xk}$  and  $F_{zk}$  produces overturning moment as the Froude- Krylov forces on the net pressure induced forces on the vertical sides and on the top horizontal surface, located on the respective centers of pressure.

Based on linear theory, the dynamic pressure due to propagating wave is given by,

$$p(x, z, t) = \frac{\gamma H}{2} \cdot \frac{\cosh k(d+Z)}{\cosh kd} \cdot \cosh(kx - \sigma t) \quad (2)$$

where,

$H$  is the wave height

$k$  is the wave number

$\sigma$  is the wave angular frequency

$Z$  is the depth

$F_{kx}$  can be obtained from  $(za)$ - area and by integrating pressure by length of the column.

Thus,

$$F_{kx} = \int_{-d}^{h-d} [p(-a, z, t) - p(a, z, t)] dz \quad (3)$$

Substituting Eq. (2) in Eq. (3) and integrating and simplifying we get,

$$F_{xk} = -2\gamma a H \frac{\sinh kh}{k \cosh kd} \sin k a \sin \sigma t \quad (4)$$

where,

$-2\gamma a H$  is a function of wave height,

$\frac{\sinh kh}{k \cosh kd}$  is a function of water depth

$\sin \sigma t$  is a function of frequency. It is constant and gives phase variation of the force.

Moment due to horizontal force

$$M_{hk} = \int_{-d}^{h-d} [p(-a, z, t) - p(a, z, t)](d - (-z)) dz \quad (5)$$

$$M_{xk} = 2a \int_{-a}^a xp[(x, (h-d), t)] dx \quad (6)$$

x is the lever arm in the above equation.

$$M_k = M_{hk} + M_{vk}$$

Approximate formulae for  $C_h$ ,  $C_v$ ,  $C_0$

$$C_h = 1 + 0.75 \left(\frac{h}{d}\right)^{1/3} \left[1 - 2.96 \left(\frac{D}{L}\right)^2\right]$$

$$C_v = 1 + 7.3 \left(\frac{D}{L}\right)^2 \left(\frac{h}{D}\right) \text{ for } \frac{\pi h}{L} < 1$$

$$C_v = 1 + 5.7 \frac{D}{L} \text{ for } \frac{\pi h}{L} > 1$$

$$C_0 = 1.9 - 1.1 \left(\frac{D}{L}\right)$$

Restrictions:  $\frac{h}{d} < 0.6$  for  $C_h, C_v, C_0$

$$0.3 < \frac{h}{d} < 2.3 \text{ for } C_h, C_v$$

$$0.6 < \frac{h}{d} < 2.3 \text{ for } C_0$$

Restrictions and approximations are based on experiments.

## 2.1.2 Morison equation

Morison equation is used to calculate the wave loads on structures in water. It is sum of two force components. Namely, inertia force of the water particles and the drag force. Water

particles in a wave carry a momentum. When the particle goes around a cylinder in water body, it accelerates first around it and then decelerates. This means work has been done on the cylinder. Meanwhile the viscous drag force is a result of separation and boundary layer friction of liquid flowing around a body placed in a flow. Morison's equation is an empirical formula. The derivation for Morison equation is based on Lectures in Hydrodynamics by Dr. T Sahoo of Indian Institute of Technology, Kharagpur, Department of Oceanography. Lecture is available of NPTEL website.

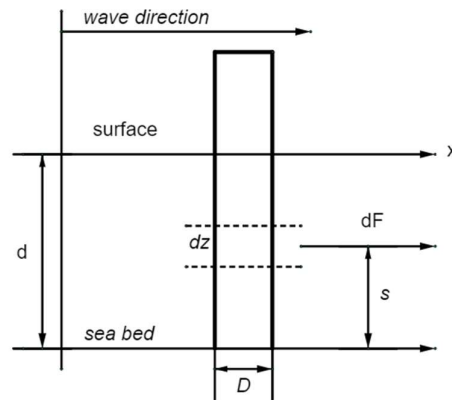


Figure 5: Fixed cylinder in Water

### Morison equation for a fixed cylinder in water

The incremental force on small segment of the cylinder  $dz$  needed to accomplish water particle acceleration at the center of the cylinder.

$$dF_i = C_m \cdot \rho \left( \frac{\pi D^2}{4} \right) \mathbf{u} dz \quad (1)$$

$dF_i$  = Inertia force on the segment  $dz$

$D$  = Cylinder diameter

$\mathbf{u}$  = Water particle acceleration

$C_m$  = Inertia coefficient ( $C_m$  is approximately 2 for uniformly accelerated)

The drag component is caused by the presence of wake on the downstream side of the cylinder. Wake is a region of low pressure.

$$dF_d = \frac{1}{2} C_D \rho D |U| U dz \quad (2)$$

$dF_d$  = Drag force

$U$  = Instantaneous particle velocity

$$U = A \sin(kx - \sigma t)$$

Combining drag and inertia components,

$$dF = [C_m \cdot p \left(\frac{\pi D^2}{4}\right) \mathbf{u} + \frac{1}{2} C_D \rho D |U| U] dz \quad (3)$$

$$F_T = \int_{-d}^0 [C_m \cdot p \left(\frac{\pi D^2}{4}\right) \mathbf{u} + \frac{1}{2} C_D \rho D |U| U] dz \quad (4)$$

(-d) approaches 0 from bottom to sea level

Where,

$$u = \frac{\pi H \operatorname{cosh}h(z+d)}{T} \frac{\sin\theta}{\sinh kd}$$

$$\mathbf{u} = \frac{-2H\pi^2 \operatorname{cosh}h(z+d)}{T^2} \frac{\cos\theta}{\sinh k} \quad (5)$$

Putting (5) in (4) and integrating we get

$$F_T = -C_m p \left(\frac{\pi D^2}{4}\right) \frac{2H\pi^2 \cos\theta}{T^2} \frac{\sinh kd}{\sinh k} + \frac{1}{2} C_D \rho D \frac{H^2 \pi^2 \sin\theta |\sin\theta|}{T^2 \sinh^2 kd} \left[ \frac{\sinh 2hd}{4k} + \frac{d}{2} \right]$$

Maximum force =  $\frac{dF_T}{d\theta} = 0$

$$\frac{dF_T}{d\theta} = C_m p \left(\frac{\pi D^2}{4k}\right) \frac{2H\pi^2}{T^2} \sin\theta + \frac{1}{2} C_D \rho D \frac{H^2 \pi^2}{T^2} \frac{2\sin\theta \cos\theta}{\sinh^2 kd} \left[ \frac{\sinh 2hd}{4k} + \frac{d}{2} \right]$$



$$\theta_{max} = \cos^{-1} \left[ \frac{-\pi D C_m}{H C_D} \frac{2 \sin^2 kd}{(\sinh kd + 2k)} \right]$$

### For flexible cylinder in waves

$$F(t) = C_{m1} \frac{\pi}{4} \rho D^2 \mathbf{u} + C_{m2} \frac{\pi}{4} \rho D^2 (\mathbf{u} - \mathbf{v}) + \frac{1}{2} C_v \rho D (u - v) |u - v|$$

Where,

$v$  is the velocity of the cylinder

$\mathbf{v}$  is the acceleration of the cylinder

$$C_{m1} = 1 - 0.12 \frac{\pi D}{L}$$

$$C_{m2} = 1.0 \quad \text{for} \quad \frac{\pi D}{L} < 0.5$$

$$C_{m2} = 1.54 - 1.08 \frac{\pi D}{L} \quad \text{for} \quad \frac{\pi D}{L} > 0.5$$

## 2.2 Sea environment

The environment where the floating wind turbine exists is influenced by the factors that will affect its operation boundary. These factors are primarily,

- Waves
- Current
- Wind

### 2.2.1 Waves: Linear wave potential theory

The basic assumptions of first order waves on potential theory are

- The fluid is inviscid
- The motion is irrotational
- The fluid is incompressible

A velocity potential  $\phi$ , is used to express the velocity vector of the fluid at any given time and space,

$$\mathbf{V} = \nabla \phi = \mathbf{i} \frac{\partial \phi}{\partial x} + \mathbf{j} \frac{\partial \phi}{\partial y} + \mathbf{k} \frac{\partial \phi}{\partial z} \quad (1)$$

Where,

$\mathbf{V}$ = Fluid velocity vector

$\phi$ = Velocity potential

$\mathbf{i}$  = Unit vector along x-axis

$\mathbf{j}$  = Unit Vector along y-axis

$\mathbf{k}$  = Unit Vector along z-axis

As the fluid is assumed to be compressible, the velocity potential has to satisfy the Laplace equation,

$$\frac{\partial^2 \phi}{\partial x^2} + \frac{\partial^2 \phi}{\partial y^2} + \frac{\partial^2 \phi}{\partial z^2} = 0 \quad (2)$$

The Laplace governing equation for  $\phi$  can be solved by applying the necessary boundary conditions. The kinematic boundary conditions and dynamic free surface conditions required for deriving the velocity potential has been given by (Faltinsen, 1999). The one scalar function required to solve the fluid pressure,  $p$ , is obtained from the Bernoulli's equation:

$$p + \rho g z + \rho \frac{\partial \phi}{\partial t} + \frac{\rho}{2} \cdot \mathbf{V} \cdot \mathbf{V} = C \quad (3)$$

Where,  $\rho$  is the fluid density and  $C$  is a random time function.

### **Kinematic boundary conditions**

For an impermeable fixed body in moving fluid,

$$\frac{\partial \phi}{\partial n} = 0 \quad (4)$$

Equation (4) means that no fluid enters or leaves the body surface. If the body is moving with velocity  $\mathbf{U}$ , it can be generalized as

$$\frac{\partial \phi}{\partial n} = \mathbf{U} \cdot \mathbf{n} \quad (5)$$

$\mathbf{U}$  can be any type of body velocity.

Let  $F(x,y,z,t)$  be the function that defines the position of a fluid particle at any point in time. Therefore, the rate of change of function  $F$  with time can be denoted as  $DF/Dt$ .

$$\frac{DF}{Dt} = \frac{\partial F}{\partial t} + \mathbf{V} \cdot \nabla F \quad (6)$$

Where  $\mathbf{V}$  is the fluid velocity at point  $(x,y,z)$  at time  $t$ . Let the free surface equation be

$$z = \zeta(x, y, z) \quad (7)$$

Where,  $\zeta$  is the wave elevation.

A fluid particle on the free surface is assumed to stay on the free surface. Therefore, following kinematic boundary condition applies on the free surface,

$$\frac{\partial}{\partial t}(z - \zeta(x,y,z)) + \nabla\phi \cdot \nabla(z - \zeta(x,y,z)) = 0$$

Or,

$$\frac{\partial \zeta}{\partial t} + \frac{\partial \phi}{\partial x} \frac{\partial \zeta}{\partial x} + \frac{\partial \phi}{\partial y} \frac{\partial \zeta}{\partial y} - \frac{\partial \phi}{\partial z} = 0, \quad \text{at } z = \zeta(x, y, z) \quad (8)$$

Here, fluid velocity  $\mathbf{V}$  in equation (6) has been expressed by velocity potential  $\phi$ .

### **Dynamic Free surface condition**

Under this condition the water pressure is equal to constant atmospheric pressure  $p_0$  on the free surface. If constant  $C$  in Equation (3) is considered to be  $p_0/\rho$ , then,

$$g\zeta + \frac{\partial \phi}{\partial t} + \frac{1}{2} \left( \left( \frac{\partial \phi}{\partial x} \right)^2 + \left( \frac{\partial \phi}{\partial y} \right)^2 + \left( \frac{\partial \phi}{\partial z} \right)^2 \right) = 0, \quad \text{at } z = \zeta(x, y, z) \quad (9)$$

The free surface conditions (8) and (9) are non linear. The problem is simplified by linearising the free surface conditions. It is assumed that there is no forward speed and the current speed is zero. The velocity potential is proportional to the wave amplitude according to the linear wave theory. The free surface condition from (7) can be transferred to  $z=0$ . Keeping the linear terms in equations (8) and (9), we get,

$$\frac{\partial \zeta}{\partial t} = \frac{\partial \phi}{\partial z} \quad \text{at } z=0 \quad (10)$$

$$g\zeta + \frac{\partial\phi}{\partial t} = 0, \quad \text{at } z=0 \quad (11)$$

Combining (10) and (11),

$$\frac{\partial^2\phi}{\partial t^2} + g \frac{\partial\phi}{\partial z} = 0, \quad \text{at } z=0 \quad (12)$$

Or,

$$-\omega^2 + g \frac{\partial\phi}{\partial z} = 0, \quad \text{at } z=0 \quad (13)$$

when velocity potential is oscillating harmonically in time with circular frequency.

### **Linear wave theory or Airy wave theory derivation.**

For this derivation, a horizontal sea bottom and a free surface of infinite horizontal extent is assumed. The free-surface condition (13) is used with Laplace equation at the following sea bottom conditions

$$\frac{\partial\phi}{\partial z} = 0, \quad \text{at } z = -h \quad (14)$$

Where h is the mean water depth.

O.M.Faltinsen derived the result for infinite water depth by assuming that the velocity potential can be represented as a product of functions, each of which depend on only one independent variable. Method of separation of variables was used to solve the Laplace equation. The following solution satisfies the Laplace Equation (Faltinsen, 1990):

$$\phi = e^{kz}(A \cos kx + B \sin kx) \cos(\omega t + \alpha) \quad (15)$$

Where,

A, B, and  $\alpha$  are arbitrary constants.

Eventually the solution for velocity potential is found to be:

$$\phi = \frac{g\zeta_a \cos(z+h)}{\omega \cos kh} \cos(\omega t - kx) \quad : \text{ For finite water depth}$$

$$\phi = \frac{g\zeta_a}{\omega} e^{kz} \cos(\omega t - kx) \quad : \text{ For infinite water depth}$$

Where,

$\zeta_a$  is the wave amplitude

$g$  is the acceleration due to gravity

$t$  is the time variabe

$h$  is the average water depth

$k$  is the wave number

$x$  is the wave propagation direction

The principles of linear theory are used to obtain a wave spectrum that defines the sea surface. A wave spectrum shows the distribution of wave energy in a sea state. The significant wave height, and spectral period are common variables. For this thesis, JONSWAP wave spectrum is used, significant wave height is taken as 4 meters and the spectral period is automatically assigned by the program.

### **2.2.2 Wind effects**

A tow operation is susceptible to local wind conditions. According to Faltinsen (1999), the wind field is assumed parallel to the surface. The average wind speed over a time period is used to calculate the effect on a structure. Wind profile is described by,

$$U(z) = U_r \frac{z^\alpha}{z_r}$$

Where,

$z$  = height above water surface

$z_r$  = Reference height (10m)

$U_r$  = Average wind velocity at reference height

$\alpha$  = height coefficient, which is obtain from standards.

### 2.2.3 Current effects

A submerged towing operation causes drag and lift forces on the tow object. A surface current has several components. They are generated by tidal, local wind, Stoke's drift, major ocean circulation, storm surges and finally local density. All these components add up to the equation, (Faltinsen,1999)

$$U = U_t + U_w + U_s + U_{ss} + U_d$$

Where,

$U_t$  is the tidal velocity component.

$U_w$  is the component from local wind.

$U_s$  is the component developed from stoke's drift.

$U_{ss}$ : component from set-up or storm surges.

$U_d$  is the component from local sea water density.

### 2.2.4 Slamming force

The high-pressure peak that is produced when the bottom of a marine structure hits the water is known as slamming force. Given the low speed and large mass coupled with small water plane area, this factor is neglected for the modelling and simulation in this thesis. None the less, it is an important aspect for marine operations. Slamming is a non-linear phenomenon and denoted by (DNV GL, 2011),

$$F_s(t) = \frac{1}{2}\rho C_s A_p (\xi - \eta)^2$$

Where,

$A_p$  is the horizontal projected area of the structure

$\xi$  vertical velocity of sea surface

$\eta$  is the vertical velocity of the structure.

$C_s$  is the slamming coefficient. It is dependent on the horizontal projected area of the structure, sea water density, height and the added mass. It is given by

$$C_s = \frac{2}{\rho A_p} \frac{dA_{33}}{dh}$$

## 2.3 Floating wind turbines

Floating wind turbines are classified into four main categories like the design classification of floating offshore structures;

1. Spar buoy type
2. Tension-leg platform type
3. Semi-submersible type
4. Pontoon type

### 2.3.1 Spar buoy type wind turbine

This kind of wind turbine consists of a floater, i.e., a floating foundation which is designed on the principles of a spar buoy and a rotor-nacelle assembly. During installation, the buoy or the floater on with the whole structure stands is towed horizontally to the assembly point in calm water. It is then up righted and stabilized with necessary ballast. A derrick crane barge is used to mount the rotor-nacelle assembly on to the floater. Later the assembled structure is towed away horizontally to the location of installation and connected to mooring systems.

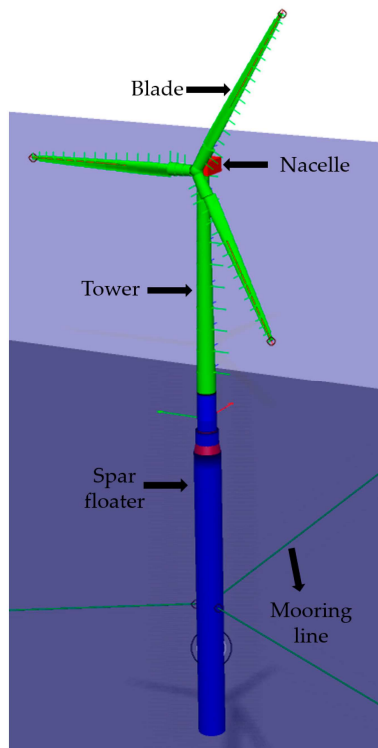


Figure 6 Spar buoy type Wind Turbine<sup>[9]</sup>

The floater is made of steel or concrete cylinders filled with ballast water and gravel to keep the center of gravity well below the center of buoyancy. This ensures that the turbine floats in the sea and stays upright by creating a large righting moment and resistance to pitch and roll motions.

The initial water ballasting was used to upright the buoy, but for permanent ballast solid iron ore, concrete or gravel is used. The permanent ballast is introduced through a chute as the water is simultaneously pumped out. Since the draft of the floating foundation is larger than the hub height above mean sea level and given the low center of gravity, the spar type wind turbines are difficult to capsize.

To keep the assembly in place, a taut, catenary spread mooring system using anchor-chains, steel cables or synthetic fiber ropes are utilized. Another option of mooring is to use a single tendon vertically held system where one line is used to hold the turbine. This system provides freedom to swivel and face the wind but at an expense of redundancy in case there is breakage of mooring lines. Single line mooring was proposed by the company SWAY.

### **2.3.2 Tension leg platform type**

In a tension leg platform type wind turbine, the turbine is mounted on a floating platform. The platform is like the one used in conventional offshore oil and gas industry. It is composed of a square pontoon with columns on which the top deck rests. For installing wind turbines, a smaller version of the same structure used in oil and gas industry is utilized, known as a mini-TLP.

This type of wind turbines can be completely assembled onshore and towed to deployment site. This reduced the cost and complexity associated with the offshore assembly as in spar buoy type wind turbines. The floating platform is held in position by vertical tethers that are anchored by either, a template foundation, suction caissons or pile driven anchors. Compared to spar buoy type or semisubmersible type, the tension leg platform type has less dynamic response to the waves.<sup>[10]</sup>



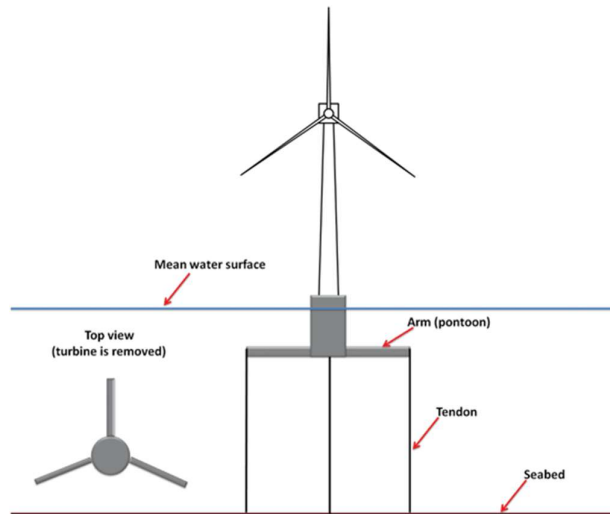


Figure 7 : Tension Leg Platform type Wind Turbine <sup>[11]</sup>

### 2.3.3 Pontoon type

A pontoon type wind turbine has a larger pontoon to carry a group of wind turbines. The large pontoon structure distributes the buoyancy and utilizes the weighted water plane area for righting moment. This helps it achieve stability. Mooring is down by conventional catenary anchor chains.

The disadvantages of pontoon type are that they are susceptible to roll and pitch motion in waves like other sea-going ship shaped vessel. Hence, they are suitable only in calm seas like a lagoon, cove or a harbor. The image below is a concept by NMRI (National maritime research institute, Japan).



Figure 8: Pontoon type wind turbines.

### 2.3.4 Semi-submersible type wind turbine

A semi-submersible type consists of a few column tubes connect to each other by other tubular members. On each of these columns or few of them, a wind turbine is attached. The columns are ballasted by partially filling them with water. This system is also called column stabilized because under afloat conditions, the water plane area of the columns provides the stability. The semi-submersible type is kept in position by mooring line. This design provides good stability and its relatively shallower draft makes it suitable for deployment in shallow-water. The design also allows for assembly onshore hence, making it relatively cheaper.



Figure 9: Semi-submersible type wind turbine (Li Liang et al).

## 2.4 Hywind Scotland wind turbines

This thesis follows the concepts and design specification of spar buoy type wind turbine Hywind. It is a floating wind turbine design on a single floating cylindrical spar buoy and is moored by cables or chains to the seabed. This design allows the structures to be placed in waters too deep for conventional bottom fixed turbines. Another favorable environmental factor is the wind. Offshore winds are typically more consistent and stronger over the sea. <sup>[12]</sup>

Statoil AS (now Equinor) designed and installed the floating wind turbines off the coast of Scotland in 2015 and has been commissioned since 2017. The main motivation behind the

design was to get over of the depth limit suffered by the regular bottom up wind turbines in offshore sector. They have a depth limitation of about 30 meters. Hence research into alternative solutions brought about this innovation.

The turbine installation used at Hywind consists of a buoyant body, a tower on the buoyant body, a generator on the tower and the generator is fitted with wind rotors. The generator itself can rotate above the tower to match the wind direction. The whole structure is kept in place by using an anchor line arrangement that consists of line connecting the tower to an anchor or on an anchor point on the seabed.<sup>[2]</sup> A ballasted catenary layout is used with three mooring cables is utilized. Each anchor cable has an extra 60 tonnes weight hanging from the midpoint to provide extra tension. The motions of the tower in wind are dampened by controlling the blade angles. This is carried out by onboard control software. The electricity produced is transmitted to shore through cables.

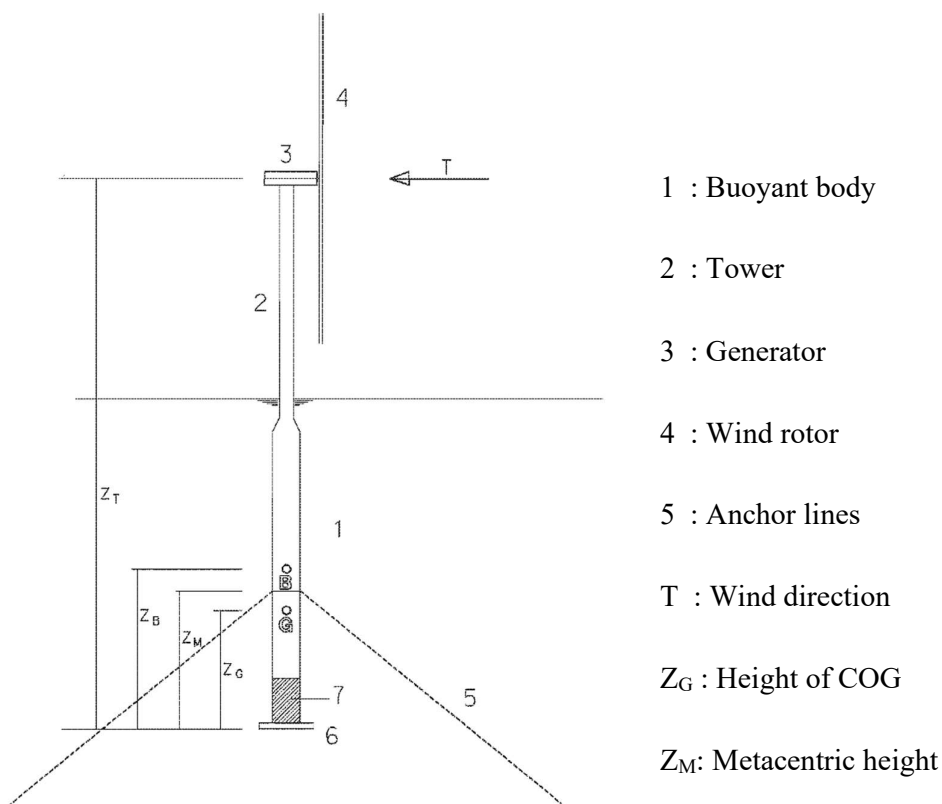


Figure 10 Hywind turbine.

1 : Buoyant body

2 : Tower

3 : Generator

4 : Wind rotor

5 : Anchor lines

T : Wind direction

$Z_G$  : Height of COG

$Z_M$ : Metacentric height

$Z_B$  : Height of Buoyancy

$Z_T$  : Tower Height

While designing something to withstand the harsh elements of sea, two factors mainly stand out. Strength of the materials used, and the cost involved. So, the floating structure is made of steel cylinder filled with ballast water and rock or iron ore. Further the cost is reduced by towing the entire assembled turbine out to the sea rather than assembling it at the point of installation. This reduced the number and cost of auxiliary support vessels involved.

The design has a draft of 85-90 meters and a displacement of about 12 000 tonnes. The diameter at water line is about 9 to 10 meters and the diameter of submerged section is around 14 to 15 meters.

To reduce risk involved and time taken for offshore operation, onshore assembly is done. The substructures are initially transported in a horizontal position to onshore assembly sites. There, the spar structures are up righted by around 8 000 tonnes of water. Once vertical, close to 5 000 tonnes of sea water is replaced by 5 500 tonnes of solid ballast.

The mooring system of the turbine utilizes a three-line mooring system. The lines are currently made of steel chains. In a wind farm with multiple turbines, common anchor points may be used. The anchoring to the seabed is done via suction anchors.

There are two characteristic movements associated with such a structure. Heave and roll/pitch. The roll is through the center of gravity of the body. In order to avoid large heave and pitch movements, the natural periods of the motions have been kept well beyond the range of waves where it has lot of energy. Each natural period has been kept at enough distance from each other to prevent the linking of the two movements.

In order to achieve high stability, large displacements and low Center of Gravity is used. This produces large corrective forces and hence small heel angles under wind load. The high stability also produces low roll period. To achieve maximum stability with satisfactory roll movement, the structure is designed so that the roll period is right above the range in which the waves have lot of energy.

To de-couple the heave and roll motions, the heave period has been set to be around 30-31 seconds, well above the roll period. To maximize the tower strength the part that passes through the water has a large diameter.

Table 2 Hywind Demo and Scotland particulars (Equinor)

<b>Dimension</b>	<b>Hywind Demo 2.3 MW</b>	<b>Hywind Scotland 6.0 MW</b>
<b>Mass</b>	5300 tonnes	11 200 tonnes
<b>Draught</b>	100 m	78 m
<b>Hub Height</b>	65 m	98 m
<b>Water Depth</b>	220 m	105 m
<b>Substructure Diameter</b>	8.3 m	14.4 m
<b>Rotor Diameter</b>	85 m	154 m
<b>Anchor</b>	Drag embedded anchor	Suction anchor
<b>Mooring System</b>	Wire/Chain	Chain

## 2.5 Marine towing operations

A large part in installation process of floating wind turbines is played by the marine towing operation wherein the fully assembled wind turbine is towed to the location of deployment. This thesis focuses most on the towing part of the operation and to be more precise its specifically deals with the towing characteristics of a spar buoy.

Marine towing operations are a wide field where the operations range from towing small pontoon to large offshore oil facilities. These vary in their location, distance and the weather needed to be traversed through. Globally shipyards are realized that modular building of ships is much more cost effective than fabricating the entire vessel structure bottom up in a single dock. This means that maybe the aft peak section of a vessel is built in South Korea, meanwhile the accommodation super structure is built in China while the whole ship is assembled in Singapore. So in cases like these the parts are brought in for assembling mainly by floating them and towing it to the destination.

A towing operation needs good planning and execution of the plan to make it a safe operation. The risks include the seasonal weather changes and human error. The risks mounted by the

weather include unexpected motions induced by waves, current and wind. Lately the modern weather forecast system has led to reduction in risk involved and fewer accidents.

A transport accident is an accident that has occurred during the towing operation or any other type of marine transportation methods. Transportation is the highest cause of accident in marine operations followed by jack-up operation. <sup>[13]</sup>

A Tow operation primarily consists of the Towing vessel, the towline and the towed vessel/ objects. Apart from the hardware, Tow plan is an important component of the operation. A tow plan is the planning and preparation before the tow commences. The process consists of. <sup>[14]</sup>

- a. Assessing the size and type of the vessel, barges, or structure to be towed and the limitations involved
- b. The tug should be of suitable size, power rating and bollard pull rating.
- c. The tow wire and other accessory are of suitable rating
- d. The passage plan should mention the safe transit times, transit through narrow bridges, river bends of heavy traffic
- e. Weather forecast for minimum of 48 hours.
- f. Noticing the depth restrictions
- g. Fuel and ration requirements
- h. Connection and disconnection arrangements for the towed structure
- i. Emergency preparedness plan.

### **2.5.1 Towline**

The most critical component in a marine towing operation is the tow rope or the towing wire or tow line. There are a few important parameters regarding towline that will help with selecting the right one for the job.

All the towing operations that doesn't involve salvage operation required only one low line. A spare towline is required by regulation on all tugs.

Bollard Pull is a measure of pulling or towing power of a vessel. It is defined as the force exerted by a vessel under full power on shore mounted rigid bollard through a tow-line.

Bollard pull is measured in kN force. It is the primary method used to measure the strength of tugboats. The vessels with highest rated BP are generally anchor handling tug supply vessels.

TBL or towline breaking load is the load limit for the towline before it breaks. DNVGL-ST-N001 provides the requirements regarding the strength of the towline.

Continues Bollard Pull	Benign Areas	Other Areas
<b>BP &lt; 40 tonnes</b>	2.0 x BP	3.0 x BP
<b>40 &lt; BP &lt; 100 tonnes</b>	2.0 x BP	(220- BP) x BP/60
<b>BP &gt; 100 tonnes</b>	2.0 x BP	2.0 x BP

*Table 3: Minimum Required Towline Breaking loads (RTBL).*

DNV also mentions the minimum required towline length. “European Formula” is used to determine the minimum deployable length of the towline. It is given by:

*For benign areas/ sheltered water*

$$L > \frac{BP}{MBL} > 1200 \text{ meters}$$

*For other conditions,*

$$L > \frac{BP}{MBL} > 1800 \text{ meters}$$

*The minimum length must be 650 meters for normal weather and 500 for benign weather.*

A modern harbor tug has a BP of over 60 tonnes and a supply vessel can provide up to 200tonnes of bollard pull.

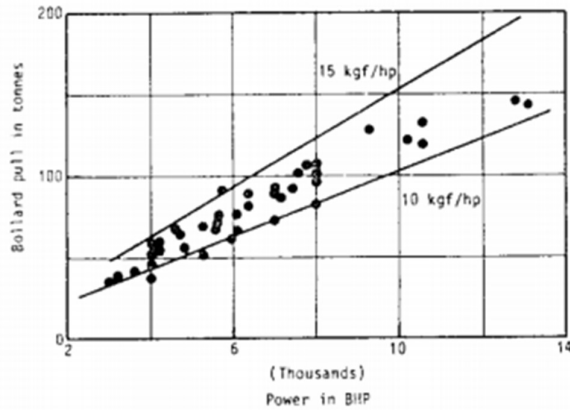


Figure 11: Supply vessel Power vs BP (Nielsen 2007).

### 2.5.2 Towing gear

The following figure represents the towing gear arrangement onboard a tug to connect to another vessel.

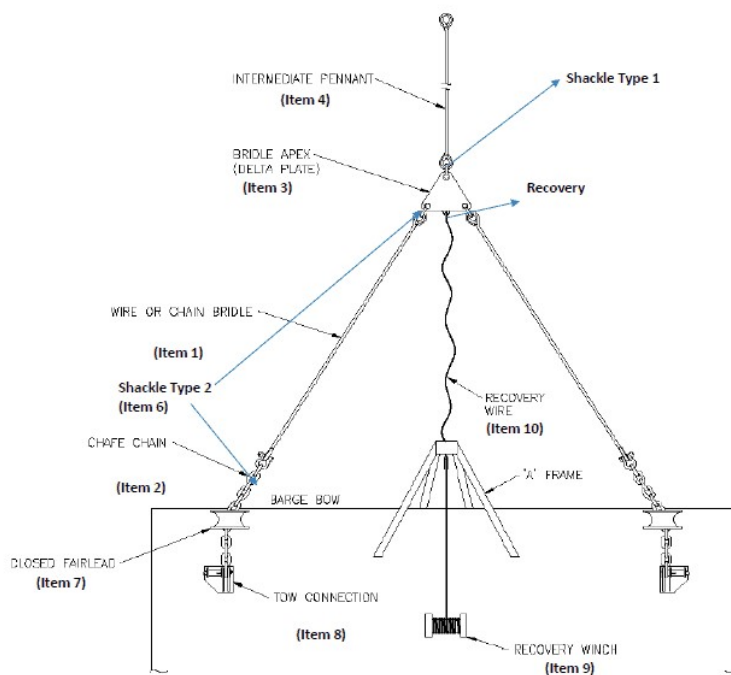


Figure 12: Tug arrangements (Navalarch.com).

In a towing arrangement there are two chains or wires connected to two points on the vessel creating a triangular shaped connection. This combination of two chains and the apex is called a towing bridle. It connects the towline to the vessel. This system is used to eliminate the



vessel sway that comes along with a single line, single point towing. The bridle system helps with better vessel control.

The method of selecting the towing equipment depends on the breaking load and the size. DNVGL-ST-001 gives the requirements for each of the item mentioned in Fig. 6.

<b>Item</b>	<b>DNVGL-ST-N001 Clause</b>
<i>Absolute minimum Deployable Towline – Length</i>	Sec 11.12.4.1 & Sec 11.13.4.2
<i>Required Towline MBL</i>	Sec 11.13.3.1
<i>Required MBL of Chafe chain (Item 2), Towing bridle leg (Item 1) and Bridle Apex (Item 3)</i>	Sec 11.13.3.4
<i>Bridle apex angle</i>	Sec 11.13.6.2
<i>MBL of intermediate wire pennant (Item 4)</i>	Sec 11.13.9.4/11.13.9.6
<i>MBL of towline shackle (Shackle type 1)</i>	Sec 11.13.8.1
<i>MBL of bridle shackle (Shackle type 2)</i>	Sec 11.13.8.2
<i>MBL of Fairlead (Item 7) and tow connection (Item 8)</i>	Sec 11.13.3.4
<i>Recovery winch capacity (Item 9)</i>	Sec 11.13.12.2
<i>MBL of recovery wire (Item 10) and Recovery Shackle (Item 11)</i>	Sec 11.13.11.5

Table 4: DNVGL-ST-N001 clauses.

**Tow connection** is the hard point where the towing bridle can be connected. Smit brackets are welded to the deck of the vessel for this kind of connection.

**Closed Fairleads or chocks** are structures welded to the vessel. They guide the chains that connect the hardpoints on the vessel to the towing bridles. The vessel hull is protected from the chain friction by chocks.

**Chain Bridle or Wire** are chains or wire that form the towing bridle. They connect the apex of the bridle and the chafe chains.

**Chafe Chain** connects the smit brackets or hard points with the towing bridle. It protects the bridle from wear and tear.

**Bridle apex** is the structure formed by connection of towing line and the towing bridles. It has three connection points, two for towing bridle and one for towline. The bridle apex has an apex angle which is the angle between two towing bridles. As per DNV requirements, it should be between 45 and 60 degrees.

**Recovery System** is used in case of breakage of towline. Winch and recovery lines are the parts of recovery system.

### 2.5.3 Propeller wash effect

Due to a short towline, the propeller wash can produce flow velocities at the tower structure which can increase the towing resistance. There are two conditions for this. One in which the transverse cross-section of the propeller wash is bigger than the dimension of the towed structure, the velocity of the propeller was may be considered as an increase in the tow velocity while calculating the towing resistance (Nielsen, 2007). Whereas in this thesis, if the dimension of the structure is larger than that the propeller wash, an estimate of the additional resistance the above method will not work. In this case the fluid flow momentum is considered.

$$\frac{dM_0}{dt} = F_p$$

$$F_p = \rho \frac{\pi D_p^2}{4} u_0^2$$

Where,

$D_p$  is the propeller outer diameter,  $F_p$  is the propeller thrust and  $u_0$  is the flow velocity assumed to be homogeneous.

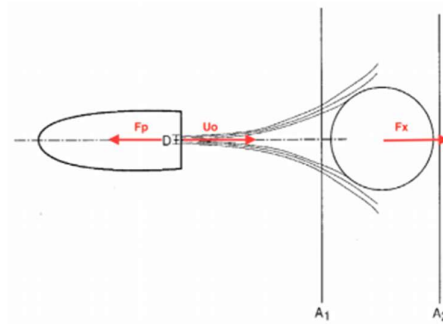


Figure 13: Propeller wash deflection (Nielsen, 2007).

The axial force on the body is given by the difference in momentum at  $A_1$  and  $A_2$ .

$$F_x = \frac{dM_{1x}}{dt} - \frac{dM_{2x}}{dt}$$

$$F_x = \rho \int_{A_1} u_x^2 dA - \rho \int_{A_2} u_x^2 dA$$

### **3 Modelling theory**

The modelling and simulation software used for this thesis is Orcaflex from Orcina LTD. There are simplifications adopted in the model which will be explained later. The various environmental parameters utilized are from DNV recommended practices. DNV-RP-C205, “Environmental Conditions and Environment Loads”, 2017 gives guidance for modelling, analysis and prediction of environmental conditions and the load acting on the structures. The recommendations are limited to loads from wind, wave and current. The recommendations are based on recent R&D developments and design experience from recent and ongoing projects. This RP gives a background information in DNV’s offshore codes. It is a supplementary to national and international regulations like NORSOK and ISO.

The other DNV recommended practices for specific marine structures and their marine loading are DNV-RP-C102, DNV-RP-C103, DNV-RP-C206, DNV-RP-F105, DNV-RP-F204 and DNV-RP-F205.

The dimensional specifications of the wind turbine are used from the data available from Equinor. It follows the dimensions of the now operational floating wind farm, Hywind Scotland.

#### **3.1 Orcaflex theory and modeling.**

Orcaflex is a software package that is used for design and analysis of a range of marine systems and their operations. The applications in offshore systems vary from riser systems to mooring systems to marine renewable and installation planning capabilities.

##### **3.1.1 Coordinate system and object connections**

Orcaflex uses multiple frames of references. Each frame of reference consists of a reference origin and a set of axial direction. Each axis represents different coordinate system. There is

one global frame of reference denoted by  $G_{XYZ}$  which has global axes in the direction,  $G_X, G_Y, G_Z$ . Then there are local coordinate systems, generally one for each object in the model denoted by  $L_{XYZ}$ . It has the axes directions of  $L_X, L_Y, L_Z$ . For lines are orientations, Orcaflex uses coordinate system of  $E_{XYZ}$ . All these systems in Orcaflex are right-handed and clockwise rotations are positive when looked at from the direction of axis of rotation. In the following figure the vessel has its own axes in the global axes.

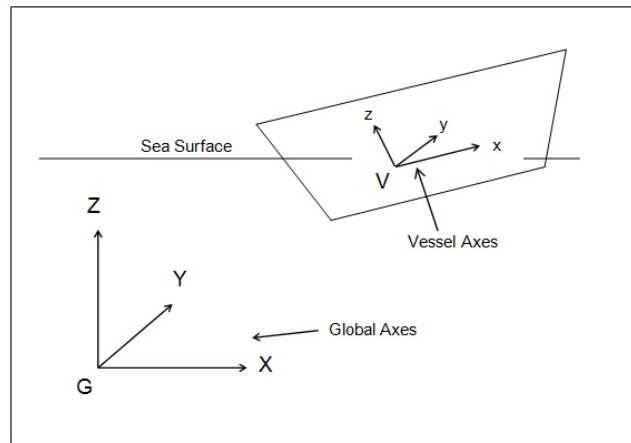


Figure 14: Coordinate system used in Orcaflex.

Data and results are displayed relative to the global axes which include data defining the sea and position of objects. The object relative items displayed commonly include the coordinate points which move with the object and the direction dependent properties of the object. Wave, current and wind directions are specified by the direction relative to the global axes

Objects can be generally fixed, anchored, free or connected to some other object as a slave. The object to which slave is connected is called master. Once the connection is made, it is treated as rigidly attached to the master object. Fixed or anchored objects remain fixed relative to the global axes all the time. Free objects have the free of movement and response to environmental loads and line loads.

### 3.1.2 Environment

Orcaflex simulation environment covers buoyancy variations with depth, water current, reaction force from the seabed and hydrodynamic loads of structures using extended form of Morison's equation. [6]

An object's buoyancy is normally assumed to be a constant with not varying much with its position. Practically though, it varies if the object is compressible due to change in volume with depth, it varies if the sea water density changes due to change in water compressibility or temperature and salinity. Normally density increases with depth. Orcaflex can model these effects on lines and buoys. The compressibility of the objects can be factored into the simulation by mentioning their bulk modulus of elasticity.

If the simulation has waves in it, currents must be extrapolated above the still water level. Orcaflex considers that the surface current applies to all the levels above the still water level. The effect of sloping seabed is not considered and is not corrected in Orcaflex. The current specified at the greatest depth is applied to all greater depths.

Seabed reaction forces affect objects like 3D buoy, 6D buoy, lines and drag chains that interact with the seabed. The seabed reaction force is the sum of penetration resistance force in the seabed in normal direction and a frictional force tangential to the seabed plane.

### **3.1.3 6D buoy theory**

In Orcaflex a 6D buoy is a rigid body with 6 degrees of freedom. They are 3 translational and 3 rotational. The equations of the motion of a 6D buoy are affected by its weight. The force is applied at its center of mass. The buoys have both mass and moments of inertia. Also forces and moments from many different effects like;

- Weight and inertial loads.
- Buoyance, added mass, damping and drag. For these, the proportion of the buoy under the water is considered.
- Slam forces when the buoy passes through the surface.
- Wing loads from a wing connected to the buoy at a specified position and orientation. Its rectangular in shape and experiences lift and drag forces.
- Loads from connected objects like link, winch or winches.

There are 3 types of 6D buoys available in Orcaflex: Lumped buoy, Spar buoys and Towed Fish. 6D buoys offer several different uses, like connecting two lines to facilitate moment transfers between lines.

### 3.1.3.1 Lumped buoy

Lumped buoys are specified without a specific geometry. This limits the accuracy of water surface interaction modelling. When a lumped buoy pierces the water surface, it is treated for buoyancy purposes as a vertical stick element with length equal to the specified height of the buoy, and hence the buoyancy variation is dependent only on the vertical position and not the orientation. This model does not have rotational stiffness experienced by most surface piercing buoys.

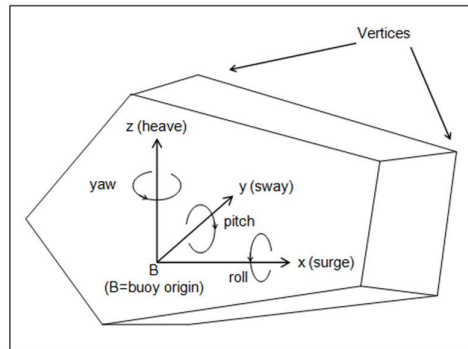


Figure 15 Lumped buoy

A lumped buoy is specified relative to its own local frame of reference  $B_{XYZ}$ . The center of Mass is specified relative to  $B_{XYZ}$ . The volume of a lumped buoy is the total volume and the center is at the center of volume which is defined relative to  $B_{XYZ}$ . The vertical dimension of the buoy is height and is used to calculate the contact area for calculating forces of contact with shapes and seabed. Height is also used to find the wetted volume for scaling the hydrostatic and hydrodynamic forces.

### 3.1.3.2 Spar buoy and towed fish buoy

A spar buoy has a body frame of reference and is built from a series of coaxial cylinders mounted along the body x-axis. The towed fish geometry is identical to spar buoy, but the orientation is along the local x-axis.

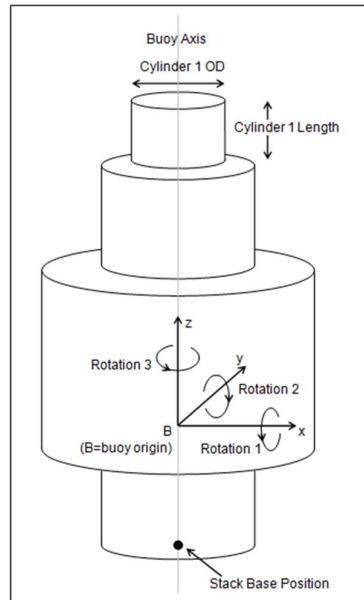


Figure 16 Spar buoy

The geometry data determines the shape of the spar buoy or the towed fish buoy. The stack shape of these cylinders determines the data used to determine the moments and forces. If the structure is water piercing, the software considers the angle of intersection between body of the buoy and the sea surface for calculating immersed volume and center of immersion volume. If the inner diameter is more than zero, then the cylinder is a hollow pipe. The hydrodynamics effects are calculated for each individual cylinder. The loads are calculated separately for each cylinder and summed to obtain the total load on the buoy.

### 3.1.4 Line theory

In Orcaflex, in order to model cables, hoses, chains etc., flexible linear elements called lines are used. They are represented by lumped mass model. The lumps of mass are called nodes and the spring joining the are called segments. Each segment represents a short piece of the line, whose properties like mass, buoyancy, drag etc. have been lumped.

Line properties are specified by dividing it into multiple user-defined sections. For each section the length and line type are defined. Orcaflex provides a “line type wizard” tool which helps set up the line types representing common structures line chains, ropes, etc.



Items that are connected to the line are called as attachments. They may be used to model clump weights, drag chains or buoyancy bags attached to the line. There are two types available, clumps are drag chains. Clumps can be buoyant or heavy. The two ends of a line are called as end A and end B are each end can be independently free, fixed, anchored or connected to a vessel, buoy, line, etc.

### **3.1.5 Dynamic analysis**

There are two approaches to dynamic analysis of a system in Orcaflex: Frequency domain and Time domain.

#### **Frequency domain**

The frequency domain solver is for solving the dynamic responses for a system at either wave frequency or low frequency. In a system subjected to first order dynamic loading defines the wave frequency response whereas a system subjected to second order dynamic loading, drift loading, and wind dynamic loading defines the low frequency response

This is a linear analysis. All nonlinearities are approximated to be linear by the process of linearization. The frequency domain can be used to solve wave frequency or low frequency solution frequencies. The results from static analysis carried out by the software is used to produce linear transfer functions that map the underlying environmental or loading process to the system's response process. Frequency domain analysis is not suitable for problems involving time dependent operations.

#### **Time domain dynamic analysis**

Time domain dynamic analysis is used for nonlinear systems. Parameters like mass, damping, stiffness, loading etc. are evaluated at each time step. It takes in account of the instantaneous, time varying geometry. OrcaFlex has two-time domain integration approaches; implicit and explicit. Both approaches use numerical time stepping algorithms to solve the equations of motion in the time domain. Initial configuration at time of the static analysis is used by the dynamic simulation and then evolves further ahead.

### 3.1.6 Object modelling

In order to analyze a system using Orcaflex software, at first a mathematical model of the practical system is created. This is done using different options in the software. The complete model consists of an environment where the objects are placed and the loads from environment are acted on the object. The objects are representative of the structures like vessels or lines or buoys that are being analyzed.

#### Vessel modelling

Vessel modelling is used to model ships, floating platforms, barges, boats etc. Their motions are prescribed by the user and are rigid bodies. The motions are be specified by time history motion data or mentioning the response amplitude operators for all the degrees of freedom. The vessels can also be driven around on the sea surface according the user input of velocities are directional headings. For this thesis, the vessel RAO are not of importance, whereas the vessel velocity is.

To create a ship, the vessel data is input into the vessel data form. The vessel can be drawn in 3D vies of the model as a wire frame or a shaded view. The initial position and orientation of the vessel is specified in terms of x,y,z connection coordinates of the vessel origin. The orientation is given by trim, heading and heel.

A vessel can different states of being. It can be either free, fixed, anchored to connected to other objects. The 'free' vessel will have full range of calculation data available. Other types will be treated as a slave or a master while will influence or restrict the vessel's calculation options.

The screenshot shows the 'Edit vessel data: vessel1' dialog box. It includes the following sections:

- Name:** vessel1
- Length (m):** -
- Type:** Vessel type1
- Draught:** Draught1
- Initial position and attitude:**

Connect to object	Position (m)			Orientation (deg)		
	x	y	z	Heel	Trim	Heading
Free	-65,4118	0,0	0,0	0,0	0,0	0,0
- Calculation:** Superimposed motion, Supports, Support coordinates, Motion elements, Air gap, Drawing, Origin drawing, Shaded drawing, Tags
- Geometry specification:** Release, Release at start of stage, Supported lines: 0
- Coordinate system:** 0
- Coordinate system table:**

No.	Name	Position (m)			Orientation (deg)		
		x	y	z	Azimuth	Declination	Gamma

Figure 17: Vessel Data Form (OrcaFlex).

## Wind turbine

The wind turbine is modelled on 6D spar buoy option available in Orcaflex. The spar buoy model is used to make the structure. It is a collection of vertically stacked cylinder of varying diameters to eventually obtain the dimensions of Hywind spar structure. The spar buoy property form gives the option of setting the base coordinates, center of mass of the object and initial inclination of the object.

A simplification has been adopted here. Since the project is about towing arrangement, actual generator and rotor effects are limited to the moment created and the wind loads on the wind at the turbine height. The moment created is simulated by having an applied load on the tower structure at the top end. For wind load while towing following formula is used as per DVN recommended practice for floating wind turbines,<sup>[7]</sup>

*“A logarithmic wind speed profile may be assumed for neutral atmospheric conditions and can be expressed as:”*

$$U(z) = \frac{u^*}{k_a} \ln \frac{z}{z_0}$$

Where,

$k_a = 0.4$  is von Karman’s constant, <sup>[8]</sup>

$z$  is the height and  $z_0$  is the terrain roughness parameter.  $z_0$  depends on wind speed for offshore locations, the upstream distance to the land, the water depth and the wave field.

Terrain type	Roughness parameter $z_0$ (m)	Power-law exponent $\alpha$
Plane ice	0.00001-0.0001	
Open sea without waves	0.0001	
Open sea with waves	0.0001-0.01	0.12
Coastal areas with onshore wind	0.001-0.01	
Snow surface	0.001-0.006	
Open country without significant buildings and vegetation	0.01	
Mown grass	0.01	
Fallow field	0.02-0.03	
Long grass, rocky ground	0.05	
Cultivated land with scattered buildings	0.05	0.16
Pasture land	0.2	
Forests and suburbs	0.3	0.30
City centres	1-10	0.40

Figure 18: Roughness parameters. <sup>[7]</sup>

The worst-case scenario is adopted here, under which it is considered that the turbine is getting head wind all the time. The variations of wind speed are of high frequency, so the net effect of wind speed variation is not consequential in overall simulation. Effective wind load on the rotor-nacelle assembly is added as an applied load in the data form for the 6D buoy.

The specifications of Hywind Scotland have been used for this thesis thereby greatly reducing the modelling time required. When the specifications are unknown, one of main task would be finding the center of mass of the structure when multiple layers of material of different density has been used as ballast inside the submerge portion. The center of mass location was roughly known from the technical report by J. Jonkman, NREL, and since the software has the option to specify the center of mass of the structure and mass, the problem can be simplified<sup>[17]</sup>.

### **Tow ropes or chains**

For this thesis the emphasis is more on the mass of the tow rope rather than the material or the thickness. Orcaflex lets the user define the section length of the line and the number of segments required. The line type wizard tool lets the user set up the line type to represent common structures like chains, ropes, etc. A line type is a collection of properties. Example, Diameter, mass per unit length and bending stiffness. The standards used here are ISO 2408:2017 and DNVGL-ST-001.

### **Deflectors**

Deflectors are essentially a tow fish buoy with a wing attached to it. It creates lift force to keep the spreader line taut. This keeps the lines with the turbines well-spaced from each other.

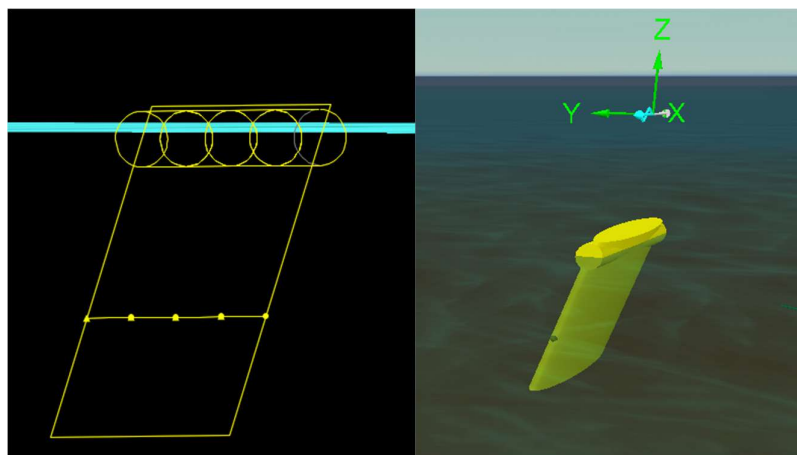


*Figure 19: Deflector.*

The deflector has three main elements modelled in it: A 6D buoy, a towed fish, which is same as a spar buoy on its side, a heavy base line to give it stability and wing to provide the lifting surface. The towed fish buoy represents the buoyancy tank.

In Orcaflex, whenever the wing is below the water surface, the lift and drag forces are calculated using the sea water density, velocity and the angle of attack. Meanwhile above the water, the same effect is calculated, but instead of sea water density, air density is applied. Since the wings do not have any mass, added mass or buoyancy, these quantities are added on to the property of the towed fish buoy.

Forces and moments on the wing is given by,

$$f_L = 1/2 \rho C_L(\alpha) a |v|^2$$

Where,

$P$  : Proportion wet of proportion of dry

$C_L$ : Lift coefficient

$\rho$  : Density of the fluid

$v$  : Relative flow velocity at the wing center

## 4 Modelling and simulation technique

### 4.1 Setup and assumptions

Primarily two scenarios are being modelled in this thesis. One of problems is study the relation of lean angle vs the tow point while all the other parameters are constant and second one is studying towline tension vs tow-speed when rest of the parameters are constant.

Following diagram shows the forces acting. In this, the spar buoy is assumed to be at constant velocity considering the large difference in mass between the tug and the buoy. The tug has only one direction of motion. Considering the waves and wind at play, this assumption will not be completely accurate. The tension of the line will be affected by heave, surge and pitch motions but only surge motion has been considered in the model.

The environmental forces act at 180 degrees in OrcaFlex coordinate system. Meaning they act head-on on the system. The effect of the wind on the rotor system has been neglected assuming that the pitch angles will be at zero and hence produce negligible effect.

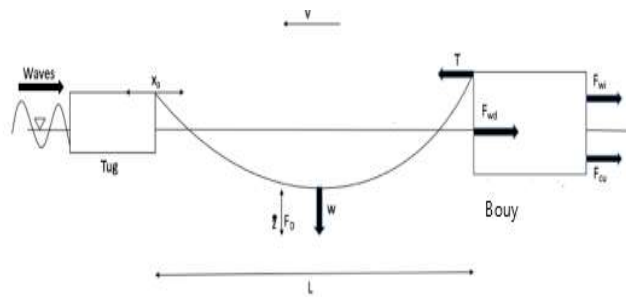


Figure 20: System model.

### 4.2 Environmental data

The environmental data in this thesis have been kept as default from Orcaflex except for Wave type. JONSWAP wave type has been taken as per the recommendation from DNV. JONSWAP is Joint North Seas Wave Observation Project. It is a wave spectrum developed on Pierson-Moskowitz spectrum. <sup>[16]</sup> The wave direction is head on at 180 degrees, the significant height is 4 meters and average wave period is 8 seconds.

The other environmental data includes the current, waves, sea water temperature, viscosity and density. The values remain constant throughout the simulation.

Parameter	Value
Wave Train Name	Wave1
Wave Type	JONSWAP
Number of Components	217
Seed	12345
Hs (m)	5
Tz (s)	10
Kinematic Viscosity (m <sup>2</sup> /s)	1.35E-03
Density (te/m <sup>3</sup> )	1,025
Depth	1000m
Current	2 m/s
Wind	20 m/s

Table 5: Environmental Parameters.

### 4.3 Spar buoy/ Floating wind turbine

The particulars of the turbine model have been obtained from Equinor website. The model has been made as close as possible dimensionally to the Hywind Scotland model. The response analysis needed to be verified for generic models. Even so, this will provide a good estimate of the response when scaled to different models.

The Substructure is a made in Orcaflex as a Spar-buoy consisting of several different stacked cylinders. The parameters of the buoy like diameter, and length of each cylinder determine the forces on it. Loads are calculated for each cylinder individually, then summed to obtain the total load on the buoy. Orcaflex calculates the hydrodynamic loads on the spar buoy using extended form of Morison's equation<sup>[17]</sup>. That is,

$$F_t = (\Delta \cdot a_f + C_a \cdot \Delta \cdot a_r) + \frac{1}{2} \cdot \rho \cdot C_d \cdot A \cdot V_r |V_r|$$

Where,

$F_t$  : Fluid Force

$\Delta$ : Fluid mass displaced

$a_f$ : Fluid acceleration relative to earth

$C_a$ : Added mass coefficient

$a_r$ : Fluid acceleration relative to body

$\rho$ : Density of fluid

$C_d$ : Drag coefficient of the body

$V_r$ : Fluid velocity relative to body

$A$ : Drag area

**Structure particulars:** The tower particulars and the subsea structure particulars have been taken off of the Equinor website and used in the construction of Hywind Scotland Wind Turbines.

Parameter	Value
Tower Diameter	7.5 m
Spar Diameter	14.5 m
Total Mass	11 200 tonnes
Center of gravity	35 m from stack base
Added mass Coefficient	1
Drag Coefficient	0.7

Table 6: Wind turbine Characteristics

### 4.3.1 Ballast mass and submerged area

Given

Total mass:  $m_t = 11\,000$  tonnes

#### Spar details

Outer diameter,  $d_{so} = 14.5$  m

Inner diameter  $d_{si} = 14.0$  m

Wall thickness  $t_s = 0.05$  m

Area  $A_s = 11.19$  m<sup>2</sup>



## Tower Details

Outer diameter,  $d_{to} = 7.5$  m

Inner diameter  $d_{ti} = 7.4$  m

Wall thickness  $t_t = 0.03$  m

Area  $A_t = 1$  m<sup>2</sup>

## Material Densities

Steel : 7 800 kg/m<sup>3</sup> , Sea Water : 1 025 kg/m<sup>3</sup>

## Submerged depth calculation

Mass of submerged spar :  $m_s = \rho_{steel} \cdot A_s \cdot l_s \approx 10\,400$  tonnes

Mass of tower :  $m_t = \rho_{steel} \cdot A_t \cdot l_t \approx 700$  tonnes

If the structure is floating, by Archimedes principle, the buoyancy will be equal to the force due to gravity. Assuming the spar structure gives all the required buoyance and all of the spar has to be immersed,

$$m_{Spar\ bouyancy} = \rho_{sea\ water} \cdot \frac{\pi}{4} \cdot d_s^2 \cdot l_s \approx 20\,400\ tonnes$$

This is clearly much more than that is required. So in practice a higher density concrete permanent ballast is used instead of sea water, thereby reducing the buoyancy to optimum level.

Ideally the spar should provide a buoyancy that is equal to the mass of the complete structure. So assuming the density of the ballast is 4 000 kg /m<sup>3</sup>,

$$11\,000 = m_{spar\ mass} = \rho_{concrete} \cdot \frac{\pi}{4} \cdot d_s^2 \cdot l_{concrete\ fill}$$

$$l_{concrete\ fill} = \frac{11\ 000}{\rho_{concrete} \cdot \frac{\pi}{4} \cdot d_s^2} \approx 17.5\ m$$

In practice multiple layers or loose ballast, high density concrete and SW is used for stabilizing the structure. The concrete is called Magna dense and is supplied by LKAB minerals.

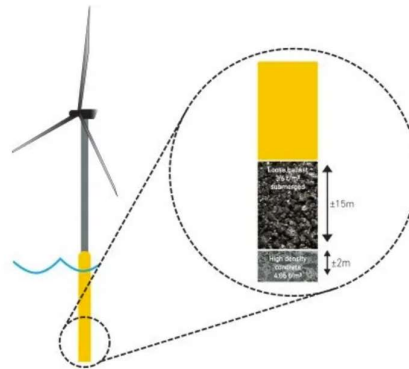


Figure 21: Permanent ballasting arrangement (LKAB minerals).

The drag coefficient was used as of a uniform cylinder. The wind load was found to be ignored at zero pitch condition; the blades have a minimum cross-sectional area.

Edit 6D Buoy Data: Wind Turbine1

Name: Wind Turbine1 Type: Spar Buoy Disturbance Vessel: None

Connections: Free Degrees of freedom included in statics: All Wave Calculation Method: Specified by Environment

Initial Position and Attitude:						Inertia:						
X (m)	Y (m)	Z (m)	Rotation 1 (deg)	Rotation 2 (deg)	Rotation 3 (deg)	Mass (t)	Mass Moments of Inertia (t.m <sup>2</sup> )	Centre of Mass (m)				
x	y	z				x	y	z	x	y	z	
-300,000	0,000	0,000	0,000	0,000	0,000	11,200E3	100,000	100,000	100,000	0,000	0,000	-40,000

Stack Base Centre Position:

x (m)	y (m)	z (m)
0,000	0,000	-70,000

Bulk Modulus: Infinitely

Cylinders:	Diameters (m)		Length (m)	Cumulative length (m)
	Outer	Inner		
1	7,500	0,000	75,000	75,000
2	8,000	0,000	10,000	85,000
3	8,500	0,000	1,000	86,000
4	9,000	0,000	1,000	87,000
5	9,500	0,000	1,000	88,000
6	10,000	0,000	1,000	89,000
7	10,500	0,000	1,000	90,000
8	11,000	0,000	1,000	91,000
9	11,500	0,000	1,000	92,000
10	12,000	0,000	1,000	93,000
11	12,500	0,000	1,000	94,000
12	13,000	0,000	1,000	95,000
13	13,500	0,000	1,000	96,000

Buttons: Give Buoy negligible properties, Support Types..., OK, Cancel, Next

Figure 22: Turbine Spar data form.

## 4.4 Towline model

### 4.4.1 Mass-Spring-Damper model of towline.

Following explains the mass spring damper model when the system has one turbine and one tug and one towline.

The towline is assumed be submerged in the water throughout the simulation. The parameters affecting the towline are its elastic stiffness and the geometric stiffness or towline stiffness. The viscous forces are represented by the damper in the parallel to the geometric stiffness

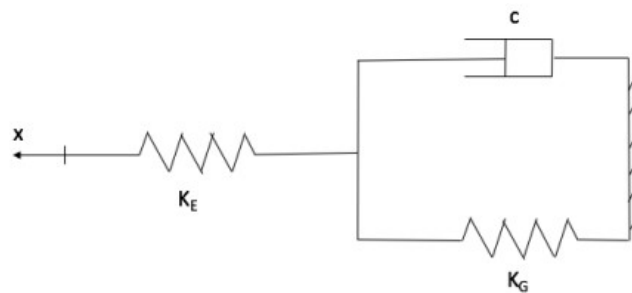


Figure 23: Mass-Spring-Damper model of a towline.

The stiffness of the line controls the low frequency motion of the tow and it controls the dynamic tension of the towline.

The towline specification were taken using the standards mentioned in section 3.1.6.3. The parameters are,

Parameter	Value
Section length	650 m
Axial Stiffness	101 000E3 kN
Poisson Ratio	0.5
Torsional Stiffness	80 000 kN.m <sup>2</sup>
Added mass coefficient	1.0
Mass	0.01 te/m
Outer Diameter	0.04

Table 7: Towline parameters.

## 4.5 Other objects

For this simulation, the vessel specifics are not important, so a generic vessel dimension has been used. The bridle system for the towing is simulated by using 3D buoy function in Orcaflex. Its mass is neglected and entered as 0.01 ton. The 3D buoy is exempted from static analysis. The bridle triangle uses lines of section length of 30 meters each with mass of 0.01 ton/meter. Remaining parameters of bridle lines are the same as towline.

## 5 Simulation and results

Three different modelling scenarios were created in Orcaflex and multiple simulations were run. The first scenario was to first the optimum tow point which produced least pitching while in towing operation. The second one was to study the variation in towing force when the tow speed increased and lastly to study the feasibility of towing multiple turbines in a single operation.

### 5.1 Tow point vs pitch angle

Different simulations were run to obtain the maximum pitch angle of the turbine structure under a towing operation. To make the simulation times smaller, instead of having a prescribed motion for the tug, the tug was assumed to be moored to a fixed point and head current of varying speed was introduced. The current variation with depth was eliminated by having only 2 profiles for the current and keeping them in the same direction as the surface current. The multiplying factor for each depth was kept 1 to keep a constant velocity throughout the profile.

Orcaflex uses a ramping function for build-up time at the beginning of simulations. This reduces the simulation time. During the build-up time, the wave dynamics, vessel motions and current are built up smoothly from zero to full value. This gives a soft start to simulation which reduces transient responses and avoids the need for long run times. The ramping factor is calculated by Orcaflex using this equation,

$$\text{Ramping factor} = r^3(6r^2 - 15r + 10)$$

Where,  $r$  is the proportion of the build-up stage completed, given by,

$$r = \frac{\text{Time} + \text{length of stage 0}}{\text{length of stage 0}}$$

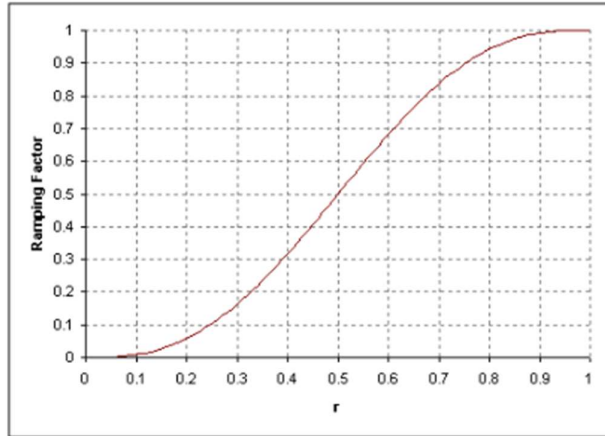


Figure 24: Ramping function (Orcina).

The remaining environmental parameters follow the DNVGL recommended practices and are of the values shown in section 4.2. The center of gravity has been considered to be at  $z = -30$  m.

## Results

Following is the sample output obtained from Orcaflex while towed from a point at the surface. All the simulation results have been added in Appendix 1.

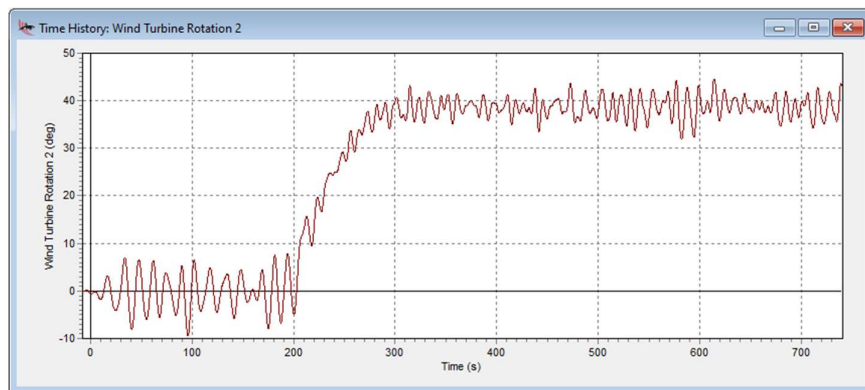


Figure 25: Graph of Turbine pitch versus time elapsed at  $z = 0$  m and sea state 6. The graph stabilizes around 290 seconds and stays at roughly 42 degrees.

All the result was tabulated and following output was seen. In this graph, the sudden rising trend of the curve beginning at 200 seconds is due to the line slack being taken up.

Two different sea states were compared for towing operation. First at sea state zero where the water is calm, has a glassy surface with zero waves. For this the wind speed was set to zero,

that is 0 Beaufort number The tow speed remained constant 2.4 m/s with 1 m/s head current. Following result was observed.

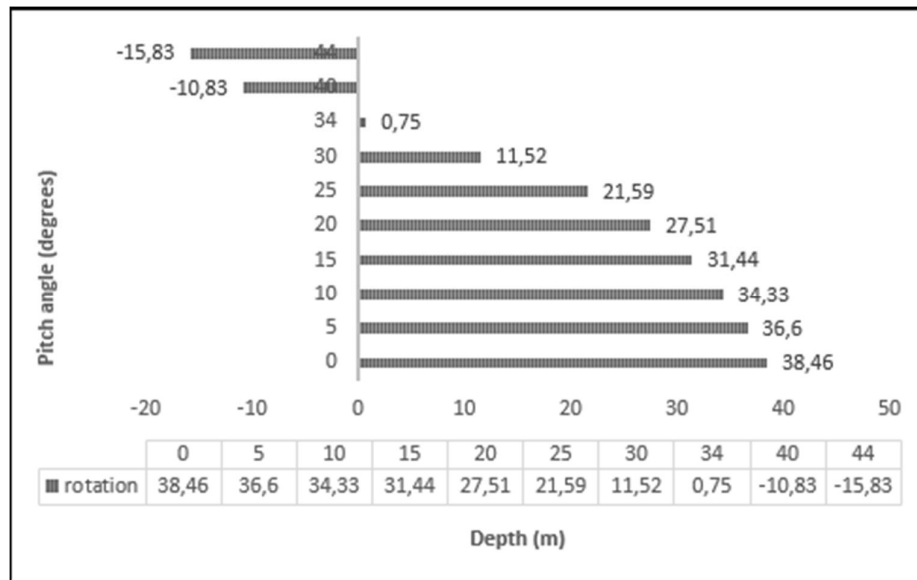


Figure 26: Comparison of Tow point vs Pitch angle at sea-state = 0.

After this a second set of conditions with parameters conforming to DNV RP was used. This would mean a ‘very rough’ sea state with WMO sea state code of 6. The wind was at 20 m/s, a ‘Gale/Fresh Gale’ or Beaufort number 8. Following was observed:

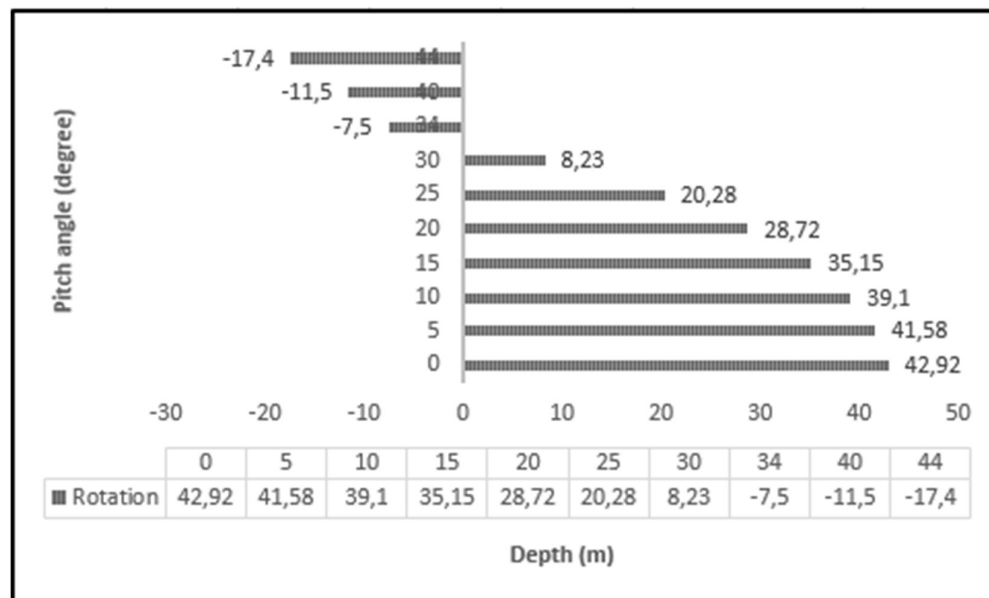


Figure 27: Comparison of Tow point Vs Pitch angle at sea state = 6

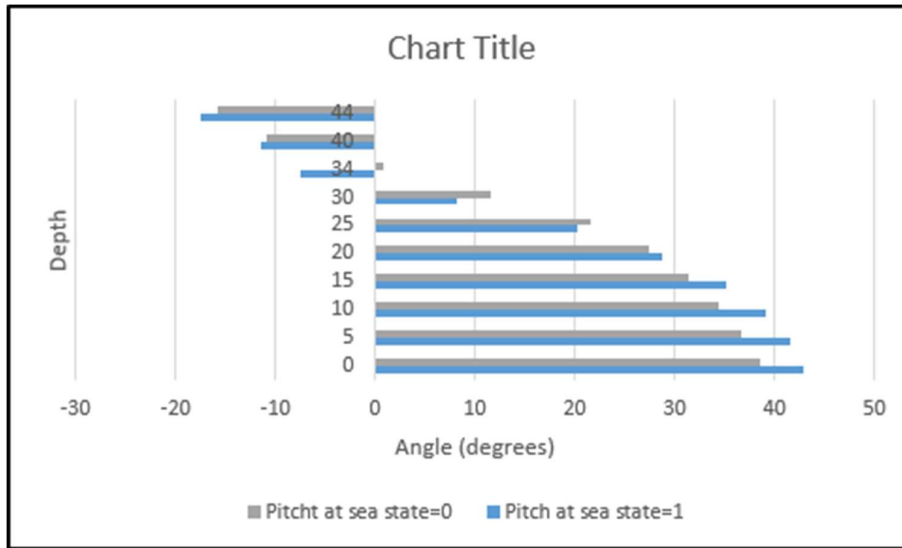


Figure 28: Sea state 0 vs Sea State 6.

In Fig. 28 we can see the difference in the pitch angles of the structure under different sea states. The farther it is towed is from the optimum point, the more the pitch angles are in rough sea state.

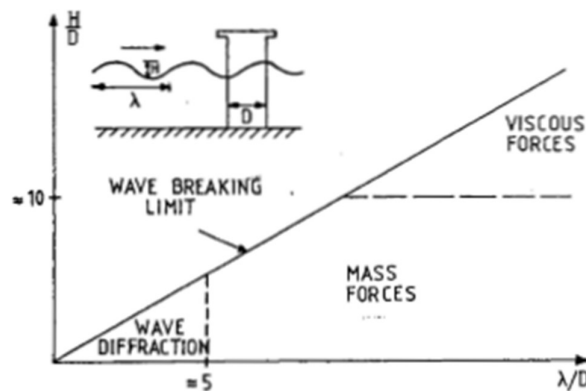


Figure 29: Comparison of mass forces, viscous drag and diffraction forces on marine structures. (Faltinsen, 1990)

In a marine structure, the wave-induced motions and loads are determined by both viscous effects and potential flow effects. A potential flow effect includes wave diffraction and radiation around the structure. Fig. 29 show the relation between the forces, sea state and structural parameters. This figure is based on effect of horizontal forces on a vertical circular cylinder standing on sea floor and penetrating the surface. The dimension of the structure used in the modelling and wavelength of 156 m (appendix 3) and wave height of 5 meters.



Therefore, the  $H/D$  and  $\lambda/D$  are respectively, roughly, 0.3 and 10. That means that the hydrodynamic forces are mainly potential flow forces with undisturbed local fluid acceleration. Both wave diffraction and viscous forces are not significant.

## 5.2 Tow speed vs line tension

The second scenario that is being investigated in this thesis is to find the scope of towing multiple turbines. For this first the towing forces due to single turbine under various speeds were checked. The following was found.

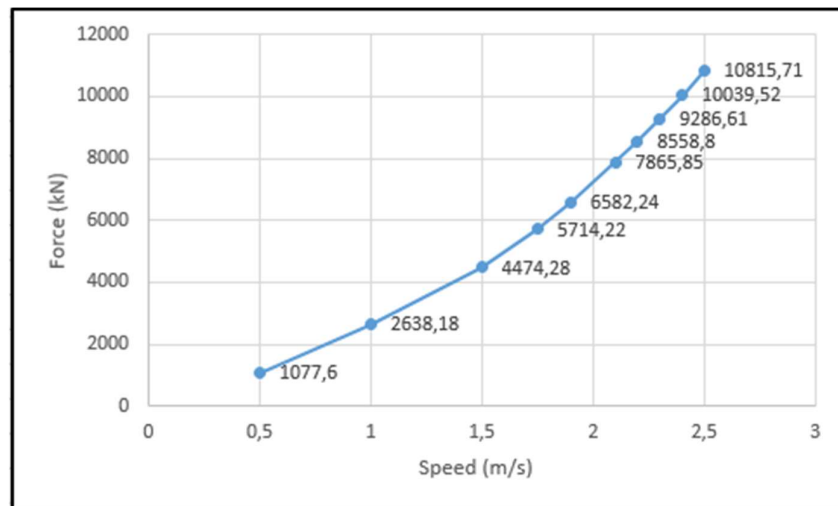


Figure 30: Tow speed vs force in the towline.

The bollard pull required increases considerably as the towing speed increases. This is already an indication that there would be an enormous Bollard pull demand for multiple turbines. Nonetheless, a scenario with parameters recommended for modelling by DNV was used to see how much force would be exerted on a towline to keep the structure in one position under a 1 m/s head on current. Following was obtained:

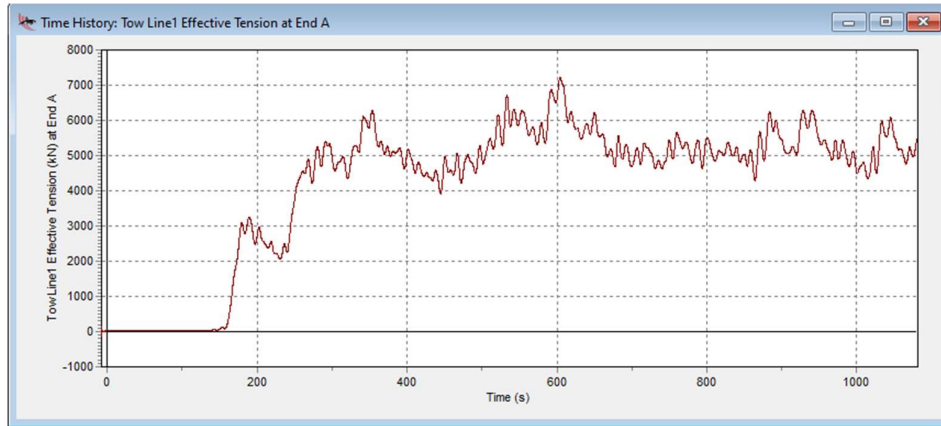


Figure 31: Tow line tension at 1 m/s speed.

The total force was found to be 5498 kN, which is approximately equal to 561 tonnes of forces. This is more than the maximum Bollard pull of the most powerful tug in existence. *Far Samson*, is a design developed by Rolls-Royce vessel owned by Farstad Shipping of Norway with a record bollard pull of 423 tonnes under testing. It must be surmised that it is not viable to carry out towing operations of multiple wind turbines.

## 6 Concluding Remarks

This report has tried to explain the work that was done in the Lab using the OrcaFlex software to model and simulation different conditions experienced by a floating turbine while undergoing towing operation. Different scenarios were considered, and results were analyzed. The report has investigated previous theoretical work done in this field as well as the future technologies being developed. The model created has been kept as close to Hywind Scotland dimensions as possible. However, lack of complete data and limitations of the software means the outputs from the simulations haven't been tested experimentally or compared to real world data.

In the current economic reality of shoestring budgets for engineering projects, every single penny counts towards design, installation and operational optimization. This thesis has tried to address this by trying to find a least damaging way to tow the turbines. It has also been found that it is unfeasible to conduct a towing operation involving multiple floating turbines of Hywind Scotland Dimensions.

The future work on this topic should be focused towards experimental validation of the simulation results with a scaled model test in a float tank. Also, more modelling and simulation work can be done for smaller turbines and the possibility of conducting towing operation involving multiple smaller. Another area to be explored in this field is the overall environmental impact of these systems during their product cycle. The product life cycle consists of maintenance operation and decommissioning as well. The Waste produced from a single decommissioned turbine is of immense scale and has a big environmental footprint. It to be seen if the economic and environmental impact of floating wind turbines are really outweighed by their benefits in long term.

## Works cited

- [1] Intergovernmental panel on climate change, ‘*Climate change 2014 Synthesis Report*’, p56
- [2] “*Floating wind turbine installation*”, Sveen et al, US Patent No. US7819073B2, 2006
- [3] Fitriadhy, Ahmad & Yasukawa, Hironori. (2016). Ship Technology Research Schiffstechnik ‘*Turning Ability of a Ship Towing System Turning Ability of a Ship Towing System*’, Ship Technology Research.
- [4] Fitriadhy, Ahmad & Yasukawa, Hironori. (2013). ‘*Course stability of a ship towing system*’. Ocean Engineering. 64. 135–145. 10.1016/j.oceaneng.2013.02.001.
- [5] James F Wilson, 2003, “Fluid load regimes”, Dynamics of offshore structure, p88
- [6] Morison J R, O'Brien M D, Johnson J W, and Schaaf S A, 1950, “*The force exerted by surface waves on piles* “. Petrol Trans AIME.
- [7] DNV-RP-C205: Environmental Conditions and Environmental loads, Recommended practices, October 2010, p16.
- [8] Huffman, G., & Bradshaw, P. (1972). ‘*A note on von Kármán's constant in low Reynolds number turbulent flows*’, Journal of Fluid Mechanics, 53(1), 45-60.
- [9] Putri, R.M.; Obhrai, C.; Jakobsen, J.B.; Ong, M.C. ‘*Numerical Analysis of the Effect of Offshore Turbulent Wind Inflow on the Response of a Spar Wind Turbine*’, Energies **2020**, *13*, 2506.
- [10] C. M. Wang, T. Utsunomiya, S. C. Wee & Y. S. Choo (2010) Research on floating wind turbines: a literature survey, The IES Journal Part A: Civil & Structural Engineering.
- [11] Karimirad M. (2014) Floating Offshore Wind Turbines. In: Offshore Energy Structures. Springer, Cham
- [12] Soukissian et al (2017). Assessment of offshore wind power potential in the Aegean and Ionian Seas based on high-resolution hindcast model results. AIMS Energy.
- [13] Lotsberg, I., Olufsen, O., Solland, G., Dalane, J. I., Haver, S. “Risk assessment of loss of structural integrity of a floating production platform due to gross errors.” Marine Structures.

[14] Tugs and tow-A practical Safety and Operational Guide, Ship Owners, 2015

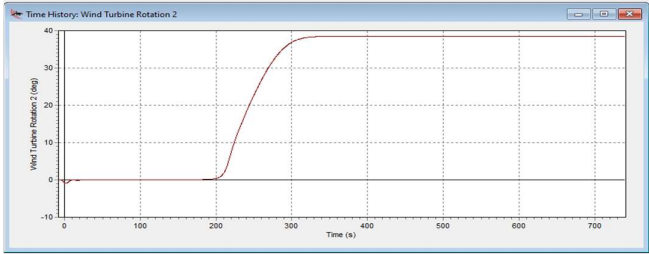
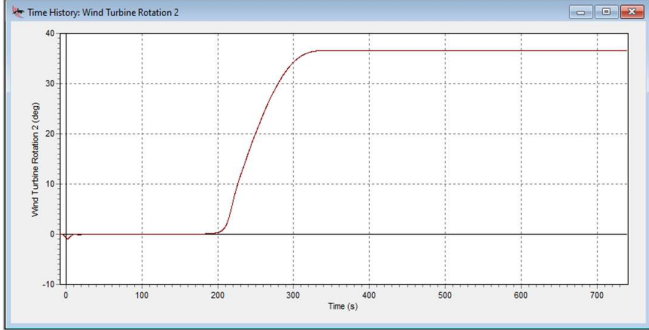
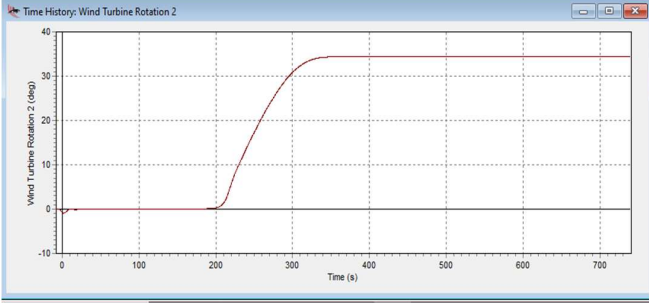
[15] <https://www.deepwind.eu/the-deepwind-project>

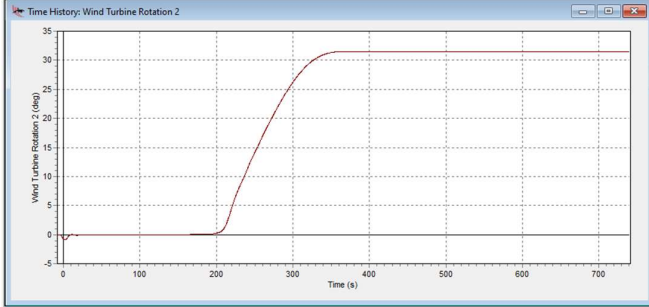
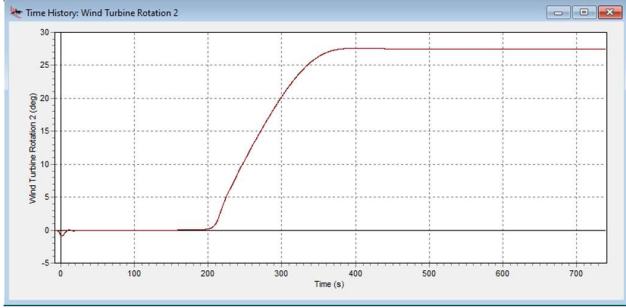
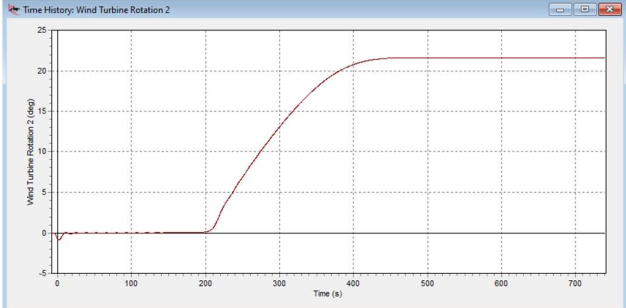
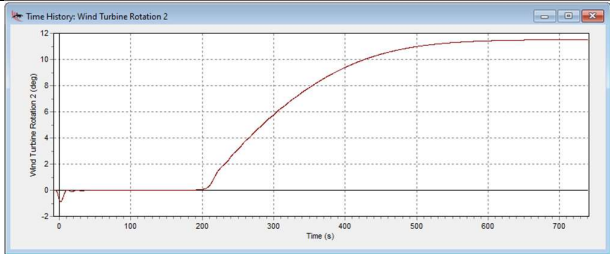
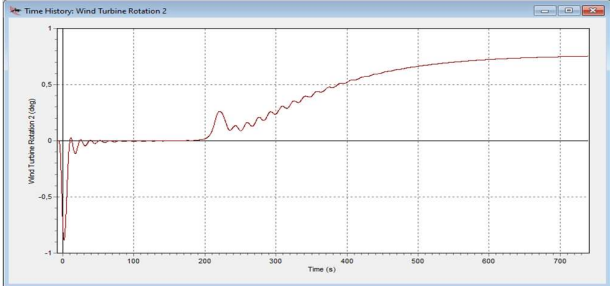
[16] Hasselmann K et al, 'Measurements of wind-wave growth and swell decay during the Joint North Sea Wave Project (JONSWAP)' Ergänzungsheft zur Deutschen Hydrographischen Zeitschrift Reihe, A(8) (Nr. 12), p.95, 1973.

[17] J.Jonk man, 'Definition of the Floating System of phase IV of OCS', Technical Report, NREL, 2010

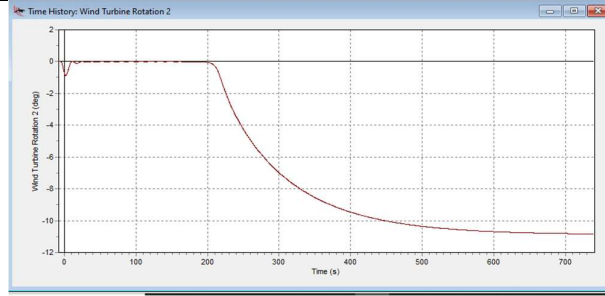
# Appendix

## 1: Turbine lean angles vs tow point at zero sea state

Depth (m)	Trend
0	
5	
10	

15	
20	
25	
30	
34	

40

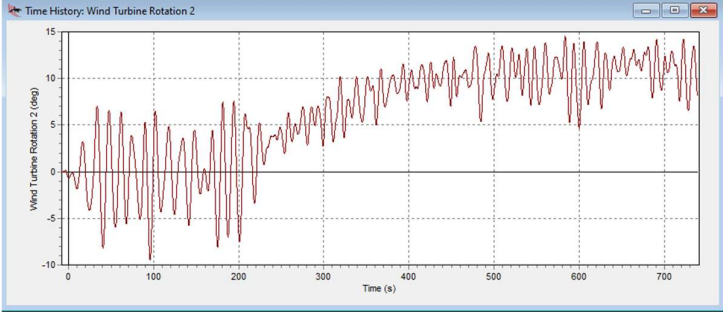
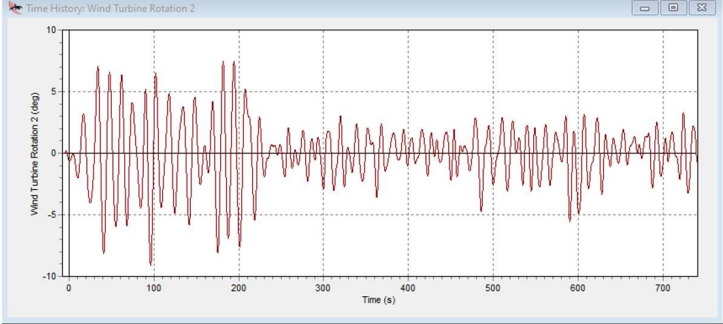
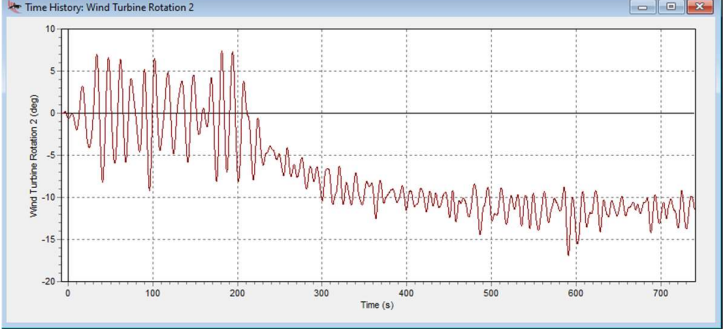
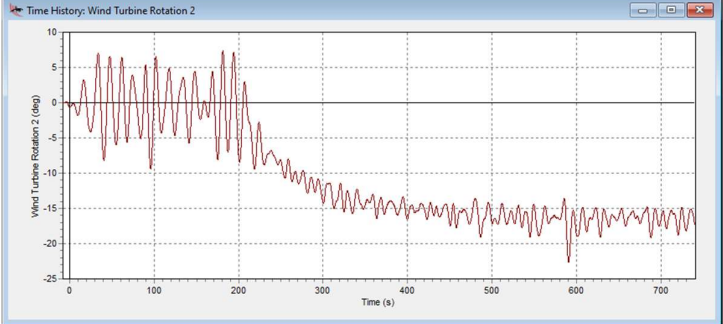


## 2: Turbine lean angle vs Tow-point in sea-state 6

Depth (m)	Trend
0	<p>A line graph titled "Time History: Wind Turbine Rotation 2". The y-axis is labeled "Wind Turbine Rotation 2 (deg)" and ranges from -10 to 50. The x-axis is labeled "Time (s)" and ranges from 0 to 700. The plot shows a red line with high-frequency oscillations. It starts near 0, has small oscillations until 200s, then rises to a mean value of about 40 degrees with large oscillations between 30 and 50 degrees from 300s to 700s.</p>
5	<p>A line graph titled "Time History: Wind Turbine Rotation 2". The y-axis is labeled "Wind Turbine Rotation 2 (deg)" and ranges from -10 to 50. The x-axis is labeled "Time (s)" and ranges from 0 to 700. The plot shows a red line with high-frequency oscillations. It starts near 0, has small oscillations until 200s, then rises to a mean value of about 40 degrees with large oscillations between 30 and 50 degrees from 300s to 700s.</p>



<p>10</p>	
<p>15</p>	
<p>20</p>	
<p>25</p>	

30	 <p>The plot shows the time history of Wind Turbine Rotation 2 (deg) over 700 seconds. The y-axis ranges from -10 to 15. The signal starts at 0, oscillates between approximately -8 and 8 degrees until 200 seconds, then drifts upwards to oscillate between approximately 5 and 15 degrees until 700 seconds.</p>
34	 <p>The plot shows the time history of Wind Turbine Rotation 2 (deg) over 700 seconds. The y-axis ranges from -10 to 10. The signal starts at 0, oscillates between approximately -8 and 8 degrees until 200 seconds, then drifts downwards to oscillate between approximately -5 and 3 degrees until 700 seconds.</p>
40	 <p>The plot shows the time history of Wind Turbine Rotation 2 (deg) over 700 seconds. The y-axis ranges from -20 to 10. The signal starts at 0, oscillates between approximately -8 and 8 degrees until 200 seconds, then drifts downwards to oscillate between approximately -10 and -18 degrees until 700 seconds.</p>
44	 <p>The plot shows the time history of Wind Turbine Rotation 2 (deg) over 700 seconds. The y-axis ranges from -25 to 10. The signal starts at 0, oscillates between approximately -8 and 8 degrees until 200 seconds, then drifts downwards to oscillate between approximately -15 and -22 degrees until 700 seconds.</p>

### 3: Wavelength for a given sea-state at a water depth 'h'

$$\omega^2 = kg \tanh(kh),$$

$$\left(\frac{2\pi}{T_0}\right)^2 = \frac{2\pi}{\lambda} (9.8) \cdot \tanh\left(\frac{2\pi}{\lambda} \cdot h\right)$$

Where,  $h$  is the depth,  $T_0$  is the period and  $\lambda$  is the wavelength.

When  $h$  approaches infinity,  $\tanh(kh)$  approaches 1.

Therefore,

$$\left(\frac{2\pi}{T_0}\right)^2 = \frac{2\pi}{\lambda} (9.8)$$

Or,

$$\lambda = \frac{g}{2\pi} T_0^2 = 156 \text{ m.}$$

